CORA Cork Open Research Archive
Cartlann Taighde Oscailte Chorcaí

Title	LC-MS/MS-based metabolite profiling and functional assessment of Hydrodictyon reticulatum as a potential source of natural therapeutics collected from the Yamuna River, India
Authors	Kumar, Dharmendra;Agrawal, Shivakar;Prajapati, Manisha;Sahoo, Sanjukta;Sahoo, Dinabandhu
Publication date	2026-04-28
Original Citation	Kumar, D, Agrawal, S, Prajapati, M, Sahoo, S & Sahoo, D 2026, 'LC-MS/MS-based metabolite profiling and functional assessment of Hydrodictyon reticulatum as a potential source of natural therapeutics collected from the Yamuna River, India', Applied Food Research, vol. 6, no. 1, 102062, pp. 1-17. https://doi.org/10.1016/j.afres.2026.102062
Type of publication	Article (peer-reviewed)
Link to publisher's version	https://www.scopus.com/pages/publications/105036632844 - 10.1016/j.afres.2026.102062https://www.scopus.com/pages/publications/105036632844?origin=resultslist
Rights	© 2026, the Author(s). Published by Elsevier B.V. This is an open access article under the CC BY license (http://creativecommons.org/licenses/by/4.0/). - https://creativecommons.org/licenses/by/4.0/
Download date	2026-11-02 05:15:16
Item downloaded from	https://hdl.handle.net/10468/18887

UCC
University College Cork, Ireland
Coláiste na hOllscoile Corcaigh

Applied Food Research 6 (2026) 102062

Contents lists available at ScienceDirect

Applied Food Research

journal homepage: www.elsevier.com/locate/afres

LC-MS/MS-based metabolite profiling and functional assessment of *Hydrodictyon reticulatum* as a potential source of natural therapeutics collected from the Yamuna River, India

Dharmendra kumar [a,b], Shivankar Agrawal [c,*], Manisha Prajapati [b], Sanjukta Sahoo [d], Dinabandhu Sahoo [b,*]

[a] *Department of Botany, Miranda House, University of Delhi, Delhi, India*
[b] *Department of Botany, University of Delhi, Delhi, India*
[c] *APC Microbiome Institute, School of Microbiology, University College Cork, Cork, Ireland*
[d] *KIIT, School of Civil Engineering, Bhubaneswar, India*

ARTICLE INFO

Keywords:
Antioxidants
Lipid
α-Glucosidase
α-Amylase
Metabolomics
LCMS/MS
FTIR
CHNS
Principal component analysis (PCA)

ABSTRACT

Hydrodictyon, a filamentous green alga, was found across multiple sites in the Yamuna River, India, during COVID-19, forming harmful algal blooms. Its potential uses remain underexplored. This study investigates the nutraceutical, antioxidant, and antidiabetic properties of *Hydrodictyon reticulatum* collected from different locations. The metabolic analysis revealed the highest concentrations of carbohydrates in Haryana (24.29 ± 0.12%), reducing sugars in Baghpat (8.41 ± 0.22%), chlorophyll a in Baghpat (0.30 ± 0.06 mg/g DW), chlorophyll b in Baghpat and Katha (0.49 ± 0.08/0.02 mg/g DW), carotenoids in Baghpat (0.39 ± 0.01 mg/g DW), and flavonoids in Baghpat (13.07 ± 0.73 mg QE/g DW). The sample from Khekra exhibited the highest protein content (5.85 ± 0.13%) and phenolic content (117.57 ± 3.94 mg GAE/g DW). Lipid content, relevant for biodiesel applications, peaked in Haryana (31.47 ± 0.87%). The strongest antioxidant responses were observed for DPPH in Katha (86.45 ± 3.73%), TAC in Katha (411.80 ± 4.23 mg TAE/g DW), and FRAP in Katha (16.97 ± 0.55 μmol TE/g DW). For antidiabetic activity, the lowest (strongest) α-glucosidase IC_{50} was recorded in Katha (0.09 ± 0.03 mg/ml), while the lowest α-amylase IC_{50} occurred in Khekra (0.13 ± 0.01 mg/ml). LC-MS/MS analysis revealed a diverse array of bioactive compounds, including lipids, sterols, flavonoids, and phenolic acids. Combined LC-MS/MS, FTIR, and CHNS analyses highlight the antioxidant, anti-inflammatory, nutraceutical, and biodiesel potential of *H. reticulatum* from the Yamuna River.

Keypoints

31.47± 0.87% lipids content makes it a prominent biosource of biodiesel production.

LC-MS/MS analysis identified diverse bioactive compounds, including lipids, sterols, flavonoids, and phenolic acids with therapeutic potential.

The α-glucosidase activity exhibited an IC_{50} value of 1.47±0.02 mg/ml, while the α-amylase activity displayed an IC_{50} value of 1.68±0.01 mg/ml. It could serve as a potential source of anti-diabetic food supplement.

1. Introduction

Algae physiology and biochemistry have been studied extensively, and microalgae cultures have been developed for human consumption (Barsanti & Gualtieri, 2022). During the last decade, algae have been utilized as nutritional and pharmaceutical compositions for humans and animals (Becker, 2013; Guil-Guerrero & Prates, 2025). Microalgae biomass is a rich source of various nutrients, including fatty acids, essential amino acids (leucine, isoleucine, valine), and carotenes (leucine, isoleucine, valine, etc.) (Matos, 2017). It is considered a potentially valuable sustainable source of biologically active compounds

* Corresponding authors.
E-mail addresses: sagrawal@ucc.ie (S. Agrawal), dbsahoo@hotmail.com (D. Sahoo).

https://doi.org/10.1016/j.afres.2026.102062
Received 15 July 2025; Received in revised form 14 April 2026; Accepted 24 April 2026
Available online 25 April 2026
2772-5022/© 2026 The Author(s). Published by Elsevier B.V. This is an open access article under the CC BY license (http://creativecommons.org/licenses/by/4.0/).

due to easy cultivation and short generation times (Bürck et al., 2025). Various algal species have demonstrated antioxidant and anti-diabetic activity, including *Acanthophora spicifera, Cystoseira compression, C. myrica, Sargassum furcatum, S. swartzii, Chlorella* sp., and *Colpomenia sinuosa* (Abo-Shady et al., 2023).

Hydrodictyon reticulatum, a freshwater filamentous green alga of the family Hydrodictyaceae, is characterized by rapid growth and tendency to form large colonies, often resulting in algal blooms in eutrophic waters. Despite its ecological significance and widespread occurrence, *H. reticulatum* remains critically underexplored for its biochemical profile and biomedical potential. Previous studies have predominantly emphasized its environmental impacts and bloom dynamics (Zhang & Luo, 2022), while its possible applications in nutraceuticals, antioxidant and antidiabetic therapies, and biofuel production have received minimal attention (Gutierrez et al., 2012; Munir et al., 2020). This represents a significant knowledge gap, as *H. reticulatum's* rapid growth rate and biomass productivity suggest untapped potential for biotechnological applications. Furthermore, environmental stressors particularly those arising from anthropogenic pollution in river ecosystems are known to modulate algal metabolism and secondary metabolite production, yet the impact of these factors on *H. reticulatum's* biochemical composition remains uninvestigated.

This study aims to comprehensively characterize the biochemical composition and bioactivity of *H. reticulatum* collected from pollution-gradient sites along the Yamuna River. The specific objectives of this study was; 1. Quantify the nutritional composition (carbohydrates, proteins, lipids, pigments) and elemental profile (CHNS analysis) of *H. reticulatum* biomass; 2. Evaluate the antioxidant capacity and anti-diabetic potential (α-amylase and α-glucosidase inhibition) of algal extracts; 3. Identify and profile bioactive metabolites using LC-MS/MS and characterize functional groups via FTIR spectroscopy; 4. Assess how environmental pollution gradients (industrial discharge, agricultural runoff, urban waste) influence the accumulation of primary and secondary metabolites; 5. Determine the nutraceutical, pharmaceutical, and biofuel potential of *H. reticulatum* as a sustainable natural resource.

We hypothesize that *H. reticulatum* biomass collected from sites with varying pollution levels will exhibit distinct biochemical profiles, with pollution-stressed samples showing elevated levels of secondary metabolites (phenolics, antioxidants) as adaptive stress responses, while also maintaining substantial nutritional value. Furthermore, we predict that *H. reticulatum* will demonstrate significant antioxidant and anti-diabetic activities attributable to its phytochemical composition, positioning it as a promising candidate for nutraceutical and pharmaceutical applications.

This study represents the first comprehensive biochemical and bioactivity evaluation of *H. reticulatum*, addressing critical gaps in the literature including first study to combine advanced analytical techniques (LC-MS/MS, FTIR, CHNS) with bioactivity assays (antioxidant, anti-diabetic) to provide a holistic characterization of *H. reticulatum*. Investigation of how anthropogenic pollution gradients in a major river system (Yamuna River during COVID-19 pandemic) influence algal metabolite profiles and bioactivity. Documentation of *H. reticulatum's* antioxidant and anti-diabetic properties, expanding beyond its traditional ecological context simultaneous evaluation of nutraceutical, pharmaceutical, and biofuel applications, establishing *H. reticulatum* as a multifunctional biotechnological resource. Unique temporal context (COVID-19 lockdown period) providing insights into algal metabolism under altered anthropogenic pressures.

By bridging the gap between ecological occurrence and biotechnological potential, this research transforms *H. reticulatum* from an understudied bloom-forming species into a promising sustainable resource for disease prevention, nutraceutical innovation, and renewable energy production. The findings will inform future cultivation strategies and valorization pathways for this and other underutilized algal species in polluted freshwater ecosystems.

The findings of this study strongly support the initial hypothesis that *Hydrodictyon reticulatum* exhibits significant biochemical variability and enhanced bioactivity in response to environmental pollution gradients. Biomass collected from sites exposed to higher levels of anthropogenic stress demonstrated elevated concentrations of secondary metabolites, including phenolics and antioxidant compounds, confirming the predicted stress-induced metabolic modulation. This aligns with the hypothesis that pollution acts as a selective pressure triggering adaptive biochemical responses that enhance the synthesis of protective metabolites. Concurrently, the algae maintained substantial levels of essential nutrients such as proteins, lipids, and carbohydrates across all sampling sites, validating the assumption that *H. reticulatum* retains strong nutritional value despite environmental stress. The observed antioxidant capacity and significant inhibition of α-amylase and α-glucosidase enzymes further corroborate the predicted anti-diabetic potential of the species, linking its bioactivity directly to its phytochemical composition as revealed by LC-MS/MS and FTIR analyses. These results collectively confirm that *H. reticulatum* is not only metabolically responsive to environmental gradients but also possesses functional compounds of nutraceutical and pharmaceutical relevance. Therefore, the study validates the central hypothesis that pollution-driven metabolic plasticity enhances the biochemical and therapeutic potential of *H. reticulatum*, supporting its development as a sustainable resource for health-related and biotechnological applications.

2. Material and method

2.1. Collection of biomass and identification

The biomass of *H. reticulatum* and water samples were collected from the Yamuna River in 23 December 2020 (winter season) at different sites, as each location possesses distinct ecological conditions and levels of pollution. Sampling sites included Haryana (28.93°N, 77.21°E), Baghpat, UP (28.91°N, 77.21°E), Katha, UP (28.53°N, 77.13°E), Khekra, UP (28.66°N, 77.30°E), and Tronica City (28.75°N, 77.24°E). Algal species were identified based on morphological characteristics using standard taxonomic literature (Guiry et al., 2014). At each location, five biological replicates were collected. Algae were harvested manually from the water surface and carefully rinsed on-site with river water to remove epiphytes, debris, and associated organisms. They were then transported to the laboratory in clean, sterile paper envelopes packed in polyethylene bags. Upon arrival, the algal biomass was thoroughly cleaned with distilled water. The samples were shade-dried till constant weight, and for long-term storage prior to biochemical and metabolomic analyses, the dried samples were preserved at -20 °C in a deep freezer. Spectrophotometric experiments were conducted using a UV-Vis spectrophotometer (DU 730, Beckman Coulter) and all analytical grade chemicals used were procured from Merck, India.

2.2. Preparation of the extract and biological activities

The complete shade-dried *H. reticulatum* biomass was ground into a fine powder using a mechanical grinder. For extraction, 1 g of the powdered sample was incubated in methanol to obtain the crude extract. The extract was concentrated by evaporating in an oven at 40°C and subsequently dried using a lyophilizer. The dried extracts were collected and stored in airtight containers at 4°C for further analysis. The yield of crude methanolic extracts varied among the sampling sites. Katha exhibited the highest extract yield (407.80 μg/g dry weight), followed by Tronica City (406.47 μg/g DW), Baghpat (401.29 μg/g DW), Haryana (398.25 μg/g DW), and Khekra (396.97 μg/g DW). These results indicate slight site-specific differences in the extractable bioactive content of *H. reticulatum* and all the experiments performed in triplicates.

2.3. Extraction of pigments

Chlorophyll pigments were extracted and quantified following the

method of Aminot and Rey (2000) with slight modifications. For each sample, 1 g of dried *H. reticulatum* was used for pigment extraction. The sample was incubated in 5 mL of 100% methanol for 30 minutes on a shaker at room temperature. The extraction was repeated in triplicate to ensure consistency and reproducibility of results.

2.4. Pigment analysis

The concentrations of chlorophyll a, chlorophyll b, and total chlorophyll were calculated using the following equation: Total Chlorophyll: 20.2 (A_{645}) + 8.02(A_{663}) Chlorophyll a: 12.7(A_{663}) -2.69 (A_{645}) Chlorophyll b: 22.9(A_{645}) - 4.68(A_{663}). Total carotenoid concentration determines by Fabrowska et al. (2018), White et al. (1963). Total Carotenoid: 1000 A_{470} - 2.27 Chl. a - 81.4 Chl. b/227.

2.5. Carbohydrates analysis

Total carbohydrate was estimated by using phenol sulfuric acid method developed by DuBois et al. (1956) using glucose as the standard. Extraction of insoluble sugar, 0.1 g of samples were treated with 1 ml of 72% H_2SO_4 (v/v) in a 50 ml beaker, agitated with a magnetic stirrer at 25°C for 50 minutes, then transferred to a 500 ml conical flask. With the addition of distilled water, make the final acid content 2.5%. The reaction flask was then hydrolyzed in an autoclave for 30 minutes at 120°C. After cooling, the samples were neutralized with NaOH. For the extraction of soluble carbohydrate 0.1 g sample was treated with 10 ml of 70% ethanol at 80°C for 2 hours. After cooling, the sample was filtered, and the residue was retreated with 70% ethanol at 80°C to complete the extraction of soluble sugars. Both filtrates were thoroughly mixed, and the volumes were normalized to 100 ml with distilled water and the final solution was used for total soluble carbohydrate assays using the phenol-sulphuric acid method. Reducing sugar content was estimated by the 3,5-dinitro salicylic acid (DNSA) method given by Miller (1959).

2.6. Total protein

Total protein was analysed according to the given protocol by Bradford (1976). For the estimation of protein 0.1 g of dried algal sample was dissolved in 100 ml of 10% NaCl, agitated for 20 minutes, and filtered using Whatman filter paper No. 1. Filtrate was used for the estimation of protein. Mix 0.25 mL of the protein-containing sample with 2.5 mL of Bradford reagent and take OD at 595 nm with the help of a UV-VIS spectrophotometer. The absorbance unit data were converted to protein concentration using a calibration curve of Bovine Serum Albumin (BSA, Cat. 97350, Sigma) as the standard. The protein concentration calibration curve was created using standards ranging from 0 to 1 mg/L.

2.7. Total lipid

Three grams of dried algal sample were used for total lipid analysis following the method of Matyash et al. (2008). The sample was homogenized and lipids were extracted using a chloroform-methanol mixture (2:1, v/v). To the homogenate, one-fourth volume of saline solution was added, and the mixture was thoroughly mixed to equilibrate. After mixing, the solution separated into two phases, with lipids accumulating in the upper organic phase, which was collected. This extraction process was repeated three times to ensure complete lipid recovery.

2.8. Total phenol

Total phenolic content (TPC) was determined by the Folin and Ciocalteu method (Agrawal et al., 2022). The phenolic content was calculated as Gallic acid equivalents mg GAE/g dry weight. 0.1 ml of sample extract was mixed with 1 ml of Folin Ciocalteu (FCR) reagent (1:2 with water) and incubated at room temperature for 5 minutes before adding 1 ml of 7% sodium carbonate solution and incubating for 90 minutes. The developed colour was measured at 750 nm.

2.9. Total flavonoid

Total flavonoid content (TFC) was determined by using the aluminium chloride colorimetric method with some modifications (Agrawal et al., 2022). 0.6 mL of the sample was combined with 0.6 ml of 2% aluminium chloride was added. After 10 minutes, 2 ml of 1 M sodium hydroxide was added to the mixture. The solution was then thoroughly mixed and incubated at room temperature for 60 minutes. Absorbance was measured at 420 nm against a blank. Quercetin was used to prepare the standard calibration curve.

2.10. DPPH radical scavenging activity

The antioxidant activity of the experimental algae was determined using DPPH (2,2-diphenyl-l-picrylhydrazyl, Cat. D9132, Sigma) radical scavenging activity (Agrawal et al., 2022). 0.1 mL of DPPH solution (dissolved in methanol) was combined with 0.4 mL of 50 mM Tris-HCl solution for this experiment. A sample concentration of 200 µL was applied. The mixture was incubated in the dark for 30 minutes before the optical density was measured at 517 nm. Furthermore, 2 mL of DPPH was utilized as a control, and ascorbic acid was employed as a standard. The antioxidant activity was calculated by using absorbance value with the addition of the sample. The following formula was used to calculate the percentage scavenging activity: DPPH scavenging activity (%) = (A_0 - A_1) / A_0 × 100 where A_0 is the absorbance of the control and A_1 is the absorbance of the sample.

2.11. Total antioxidant activity

Total antioxidant activity was estimated according to the protocol of (Anjali et al., 2019). A 100 µL of the sample solution was prepared with 1 mL of combined reagent mixture (0.6 M sulfuric acid, 28 mM sodium phosphate, and 4 mM ammonium molybdate). Then, it was kept in a boiling water bath at a temperature of 90°C for 60 min. When the sample come to room temperature, the optical density of the solution was measured at 695 nm. The blank solution was prepared with those reagent solutions and methanol. The antioxidant capacity of unknown samples expressed as ascorbic acid equivalents.

2.12. Ferric reducing antioxidant power assay (FRAP)

The antioxidant activity of the extract was also evaluated by FRAP assay by monitoring the reduction of Fe^{3+}-TPTZ to blue-coloured Fe^{2+}-TPTZ (Firuzi et al., 2005). FRAP working solution was prepared by mixing 10 volumes of 300 mM acetate buffer (pH 3.6), 1 volume of 10 mM TPTZ (dissolved in 40 mM HCl), and 1 volume of 20 mM ferric chloride hexahydrate. An aliquot of 60 µL of extract at different concentrations from 50 to 2000 µg mL^{-1} was mixed with 275 µL of freshly prepared and preheated FRAP solution in a test tube. The absorbance of each sample was recorded at 593 nm after 30 min of incubation in the dark. FRAP values were expressed as micromoles of Trolox equivalents per gram of sample dry weight (µmol TE g^{-1} DW). Calibration $y = 0.464x - 0.0114$, $R^2 = 0.9996$, where x is the absorbance at 593 nm and y is the concentration of $FeSO_4.7H_2O$.

2.13. ABTS radical scavenging activity

ABTS radical scavenging activity of algal extracts were estimated according to the protocol given by Re et al. (1999). A stock solution of ABTS (Cat.A1888, Sigma) was prepared by combining equal volumes of 7 mM ABTS solution and 2.45 mM potassium persulfate solution,

followed by a 12-hour incubation at room temperature in the dark to generate a coloured solution containing ABTS·+ radicals. The working solution was prepared fresh before each test by diluting the stock solution by mixing the stock solution with 50% methanol to give an initial absorbance of 0.700 ± 0.02 at 745 nm, with the Adjust the temperature to 30°C. The free radical scavenging activity was evaluated by mixing 30 µl of different fractions (different concentrations in the respective solvent) with 300 µl of ABTS working standard solution. The decrease in absorbance was measured after 6 min at 30°C. Quercetin was used as a positive control. Scavenging activity was estimated based on the percentage of ABTS base retained according to the following formula:

$$\% \text{ Recovery} = \frac{\text{Ao} - \text{As}}{\text{Ao}} \times 100$$

where A_0 is the absorbance of the reference, A_S is the absorbance of the extract.

Antioxidant value is expressed as half-maximal inhibitory concentration (IC_{50}), the amount of antioxidant required to reduce the initial ABTS concentration by 50%. The IC_{50} value was calculated from the regression equation between sample concentration and inhibition rate.

2.14. Nitric oxide (NO) scavenging activity

A previously published method was used to test the scavenging activity of the extract on nitric oxide (NO) with a slight modification (Jagetia et al., 2004; Kumar et al., 2015). The reaction solution (100 µl) contained 10 mM sodium nitroprusside in phosphate-buffered saline (PBS, pH 7.0) and was reacted with 10 µl of the extract at varying concentrations. The reaction mixture was incubated at 37°C for 1 hour. Then, 50 µl of the reaction mixture was mixed with 50 µl of Griess reagent, and the absorbance was measured at 540 nm. The percent inhibition of NO produced was calculated by comparison with the absorbance value of the negative control (10 mM sodium nitroprusside and PBS). BHA was used as a positive control. Finally, the IC_{50} value is calculated.

2.14.1. α-amylase activity inhibition assa

The analysis of α-amylase inhibition was performed according to the method described by Kumar et al. (2023). The absorbance of the reaction mixture was measured at 540 nm using a multiplate reader (Multiska Thermo Scientific, version 1.00.40). Acarbose (1 mg/ml, Cat. 65457, SRL) was used as the standard. No testing (extraction) was required, the substance was prepared in parallel as a control and each experiment was performed three times. Results are expressed as percentage inhibition, calculated according to the formula:

$$\text{Inhibitory activity} = 1 - \frac{As}{Ac} \times 100$$

where A_s is the absorbance in the presence of the test substance, and A_c is the absorbance of control

2.14.2. α-glucosidase inhibitory activity

The α-glucosidase inhibitory activity of the extract was performed according to the method described by Kumar et al. (2023). The absorbance of the final reaction mixture was measured at 405 nm using a multiplication table reader. Results were expressed as percentage inhibition, calculated according to the formula

$$\text{Inhibitory activity} = 1 - \frac{As}{Ac} \times 100$$

where As is the absorbance in the presence of the test substance, and Ac is the absorbance of control.

2.15. Ash content

The ash content was measured by a gravimetric method using AOAC (2000) (International 1996) by burning 1 g of the sample taken in a silica crucible and kept in a muffle furnace at 575°C for 4 h. After burning, the content was cooled, weighed, and expressed in terms of percentage.

2.16. Metabolite profiling using LC–MS/MS

For the analysis of some major metabolites found in algal biomass, 1 g of dried, frozen algal biomass was crushed and extracted in triplicate by shaking at 200 rpm with 5 mL of 80% HPLC-grade methanol. The extracts were centrifuged at 6000 rpm for 15 minutes at 4 °C, and the supernatants were dried using a rotary evaporator at 50 °C. Dried residues were reconstituted in 1 mL of HPLC-grade methanol and filtered through a 0.22 µm syringe filter. Filtered extracts were pooled, and 200 µL of the combined solution was transferred to amber glass vials and stored at 4 °C as described by Mhlongo et al. (2020).

LC–MS analysis was performed using an Agilent G6549A LC-HRMS Q-TOF system (Agilent Technologies, Singapore). The instrument was equipped with electrospray ionization (ESI) and atmospheric pressure chemical ionization (APCI) sources. The mass accuracy was maintained at >2 ppm, with a resolution of 20,000. The HPLC system operated at a pressure of up to 600 bar, while the mass spectrometer was maintained under high vacuum conditions (10^{-4} to 10^{-5} Torr). A Hypersil Gold C18 column (2.1 mm × 100 mm, 1.9 µm particle size) was employed for chromatographic separation, maintained at 35 °C. The mobile phase consisted of Buffer A (0.1% formic acid in water) and Buffer B (100% acetonitrile, Cat. 24899 SRL), with a flow rate of 0.300 mL/min. The injection volume was 10 µL, and the total method run time was 25 minutes. The mass spectrometer operated in both positive and negative ion modes using full MS-data-dependent MS-$ddMS^2$ scanning. The scan range was set from 100 to 1200 m/z, with a resolution of 70,000 for full MS and 35,000 for $ddMS^2$. The AGC target was 1e6 for full MS and 1e5 for $ddMS^2$. Other instrument settings included a sheath gas flow rate of 30 (arbitrary units), auxiliary gas flow rate of 10, capillary voltage of +4.0 kV (positive mode) and –3.5 kV (negative mode), capillary temperature of 275 °C, probe heater temperature of 320 °C (positive) and 300 °C (negative), and an S-Lens RF level of 50. Raw LC-MS data were processed and analyzed using Thermo Fisher Scientific's Compound Discoverer 3.3 software.

2.17. Characterization of biomass

2.17.1. CHNS analysis

The elemental composition (carbon, hydrogen, nitrogen, and sulfur) of sun-dried biomass was determined using an elemental analyzer (Elementar Vario EL Cube, Frankfurt, Germany). The system equipped with a high-temperature combustion unit capable of complete sample digestion at temperatures up to 1,200°C (with localized temperatures reaching approximately 1,800°C at the point of combustion when tin foil was used). The system employed jet injection of oxygen to ensure efficient combustion and complete recovery of elements, including samples that are typically difficult to combust. Gas separation was achieved using purge-and-trap chromatography with multiple gas-selective columns, allowing sequential release of gases only after baseline stabilization of preceding peaks, thereby ensuring optimal peak resolution and minimizing overlap. Detection was performed using a thermal conductivity detector (TCD) for primary elemental analysis, with optional infrared (IR) detection for sulfur and oxygen, and an electrochemical detector for chlorine analysis. The instrument was equipped with an integrated autosampler (60–120 positions) for solid and liquid samples, with the capability for continuous reloading during operation. The system operated using helium or argon as carrier gases and oxygen as the combustion gas. Instrument control and data acquisition were managed via dedicated software with LIMS integration, enabling automated and

unattended operation. Approximately 1 mg of sample was encapsulated in a soft tin container and introduced into a quartz reactor containing copper oxide and electrolytic copper. The reactor was heated to 95°C, and a controlled amount of oxygen was injected to facilitate combustion. The resulting gases produced from sample oxidation were quantified by the instrument's built-in detector.

2.17.2. Fourier-Transform Infrared (FTIR) analysis

FTIR spectra were recorded using a Nicolet iS50 FTIR spectrometer (Thermo Scientific, USA) equipped with a built-in mid- and far-infrared diamond attenuated total reflectance (ATR) accessory. The system included an automated beamsplitter exchanger (ABX), a He–Ne laser, and a diamond crystal ATR platform. Detection was carried out using a tri-detector system comprising a DLaTGS detector with a KBr window, enabling high sensitivity across a wide spectral range. Spectral measurements were carried out over the range of 500–4000 cm^{-1} at a resolution of 0.5 cm^{-1}. Atmospheric correction was applied, and all analyses were performed at room temperature (25°C)

2.18. Statistical analysis

Statistical analysis was conducted using OriginPro 9.0 for Principal Component Analysis (PCA) and IBM SPSS Statistics version 28.0 for one-way ANOVA. Data were normalized and post-hoc comparisons were performed using Duncan's multiple range test. Multivariate statistical methods, including Principal Component Analysis (PCA), Hierarchical Cluster Analysis (HCA), and box plot analysis, were employed to assess correlations, variance, and relationships among variables within the dataset. Additionally, one-way Analysis of Variance (ANOVA) was conducted to evaluate the significance of differences among sample groups. Statistical significance was considered at $p < 0.05$.

3. Results

3.1. Metabolic analysis of hydrodictyon collected from different locations of Yamuna River

Metabolic analysis of *Hydrodictyon* shows the variation in the content of total carbohydrates, protein, lipids, reducing sugar, DPPH activity, total antioxidant activity (TAC), pigments, and ash content. Carbohydrate content ranged from 17.55 ± 0.63% in Khekra to 24.29 ± 0.12% in Haryana, indicating a clear site-specific variation in primary energy reserves. Baghpat (21.8 ± 0.23%) and Katha (20.27 ± 0.47%) displayed intermediate carbohydrate levels, while Tronica city recorded 19 ± 0.34%. Reducing sugar content was highest in Baghpat (8.41 ± 0.22%), followed by Katha (5.79 ± 0.29%), Haryana (5.72 ± 0.38%), and Tronica city (5.38 ± 0.30%), with the lowest value observed in Khekra (4.36 ± 0.65%). (Table 1, Fig. 1c). Protein content varied modestly among sites, with the highest concentration in Khekra (5.85 ± 0.13%) and the lowest in Tronica city (5.32 ± 0.42%). Haryana, Baghpat, and Katha exhibited intermediate protein levels of 5.37 ± 0.57%, 5.81 ± 0.10%, and 5.42 ± 0.12%, respectively. Lipid content, indicative of biofuel potential, was maximal in Haryana (31.47 ± 0.87%), followed by Katha (26.92 ± 0.78%), Baghpat (25.33 ± 0.56%), Tronica city (18.33 ± 1.23%), and minimal in Khekra (16.40 ± 0.38%) while Ash percentage, representing mineral accumulation, was highest in Tronica city (46.5 ± 1.35%) and lowest in Baghpat (14 ± 0.67%), with intermediate values in Khekra (37.5 ± 0.55%), Katha (36.4 ± 0.70%), and Haryana (27 ± 1.41%) (Table 1, Fig. 1a). Phenol content was found a maximum of 117.57 ± 0.94 mg GAE/g dry wt. at Khekra followed by 95.94±0.53 mg GAE/g dry wt., at Baghpat, 92.72±0.12 mg GAE/g dry wt. at Katha and a minimum of 81.86 ±0.87 mg GAE/g dry wt.at Tronica city followed by 84.22±0.1. 02 mg GAE/g dry wt. at Haryana collected biomass. (Table 1, Fig. 1c). Flavonoid content of 13.7±0.734 mg QE/g dry wt. was found at maximum in the biomass of Baghpat followed by 12.71± 0.36 mg QE/g dry wt. Haryana, 11.62± 0.67 mg QE/g dry wt. at katha while a minimum of 9.18 ±0.98 mg QE/g dry wt. at the Tronica city site followed by Khekra 10.96± 1.43 mg QE/g dry wt. (Table 1, Fig. 1c). FRAP found maximum 16.97±0.55 µmol TE/ g DW at Katha while NO IC_{50} 2.55±0.06 (mg/ml) found maximum at Baghpat while ABTS IC_{50} 1.66±0.16 mg/ml found maximum at Katha. (Fig. 1d). Antidiabetic potential i.e., α-amylase IC_{50} 1.68±0.01mg/ml at katha while α-glucosidase IC_{50} 1.47±0.02mg/ml found maximum at Baghpat. (Fig. 1e). Chlorophyll a content Chl. a 0.30±0.65 (mg /g DW), Chl. b 0.49±1.08 (mg /g DW) and carotenoid 0.39±1.11 (mg / g DW) found maximum in the biomass of Baghpat while total chlorophyll 0.50±0.78 (mg / g DW) found maximum in biomass collected from Katha (Table 1, Fig. 1b). DPPH radical scavenging activity was 85.93 ±2.731% and total antioxidant activity were 411.80 ± 0.982 mg TAE/ g dry wt. found maximum in the sample collected from Katha (Table 1, Fig. 1c). Ash content represents the total mineral content and was found maximum of 58.5±0.35% at Tronica city followed by 55.6±0.70% at Katha while a minimum of 14.0±0.0% at Baghpat followed by 27±1.41% at Haryana (Table 1, Fig. 1a).

Table 1
Levels of metabolites found in *Hydrodictyon* biomass collected from various locations.

Metabolites	Haryana	Baghpat	Katha	Khekra	Tronica city
Carbohydrates %	24.29 ±0.12	21.8 ±0.23	20.27 ±0.47	17.55 ±0.63	19±0.34
Reducing sugar %	5.72 ±0.38	8.41 ±0.22	5.79 ±0.29	4.36 ±0.65	5.38 ±0.30
Protein %	5.37 ±0.57	5.81±0.1	5.42 ±0.12	5.85 ±0.13	5.32 ±0.42
Lipid %	31.47 ±0.87	25.33 ±0.56	26.92 ±0.78	16.4 ±0.38	18.33 ±1.23
Ash content %	27±1.41	14±0.67	36.4 ±0.70	37.5 ±0.55	46.5 ±1.35
Chl. a mg/g	0.25 ±0.03	0.30 ±0.06	0.29 ±0.06	0.24 ±0.04	0.26 ±0.01
Chl. b mg/g	0.42 ±0.07	0.49 ±0.08	0.49 ±0.02	0.41 ±0.01	0.44 ±0.06
Total Chl. mg/g	0.35 ±0.04	0.41 ±0.09	0.50 ±0.07	0.32 ±0.05	0.36 ±0.06
Carotenoids mg/g	0.33 ±0.02	0.39 ±0.01	0.38 ±0.02	0.29 ±0.04	0.32 ±0.05
Phenol mg GAE/g DW	84.22 ±2.10	95.94 ±3.53	92.72 ±4.12	117.57 ±3.94	81.86 ±2.87
Flavonoid mg QE/g DW	12.71 ±1.36	13.07 ±0.73	11.62 ±0.67	10.96 ±1.43	9.18 ±0.98
% DPPH Activity	70.68 ±3.32	82.18 ±2.15	86.45 ±3.73	83.79 ±5.84	85.36 ±3.28
TAC mg TAE/g DW	402.25 ±5.19	405.29 ±4.16	411.80 ±4.23	400.97 ±4.04	410.47 ±3.12
FRAP µmol TE/g DW	6.13 ±0.11	15.82 ±0.20	16.97 ±0.55	3.46 ±0.11	14.71 ±0.45
ABTS IC_{50} (mg/ml)	0.97 ±0.11	0.88 ±0.13	1.66 ±0.16	0.76 ±0.11	0.75 ±0.12
NO IC_{50} (mg/ml)	1.6±0.16	2.55 ±0.06	2.1 ±0.083	1.28 ±0.27	0.89 ±0.10
α-amylase IC_{50} mg/ml	1.63 ±0.02	1.35 ±0.02	1.68 ±0.01	0.13 ±0.01	0.14 ±0.02
α-glucosidase IC_{50} mg/ml	0.37 ±0.02	1.47 ±0.02	0.09 ±0.03	0.63 ±0.01	0.22 ±0.07

3.2. Metabolic profiling of Hydrodictyon sp

Metabolomic profiling of *Hydrodictyon* sp. extract revealed a diverse array of bioactive metabolites as shown in Table 2. Key compounds such as Pheophorbide-a and Enigmol are linked to anticancer and antioxidant activities. Lipid-derived metabolites, including 1-[11Z,14Z-eicosadienoyl]-2-dodecanoyl-glycero-3-phospho-[1′-sn-glycerol], Hexadecasphinganine, and Hexadecyl Acetyl Glycerol, indicate active membrane remodelling and intracellular signalling. Choline and 12,13-DiHOME suggest roles in lipid metabolism and mitochondrial function. The detection of neuroactive

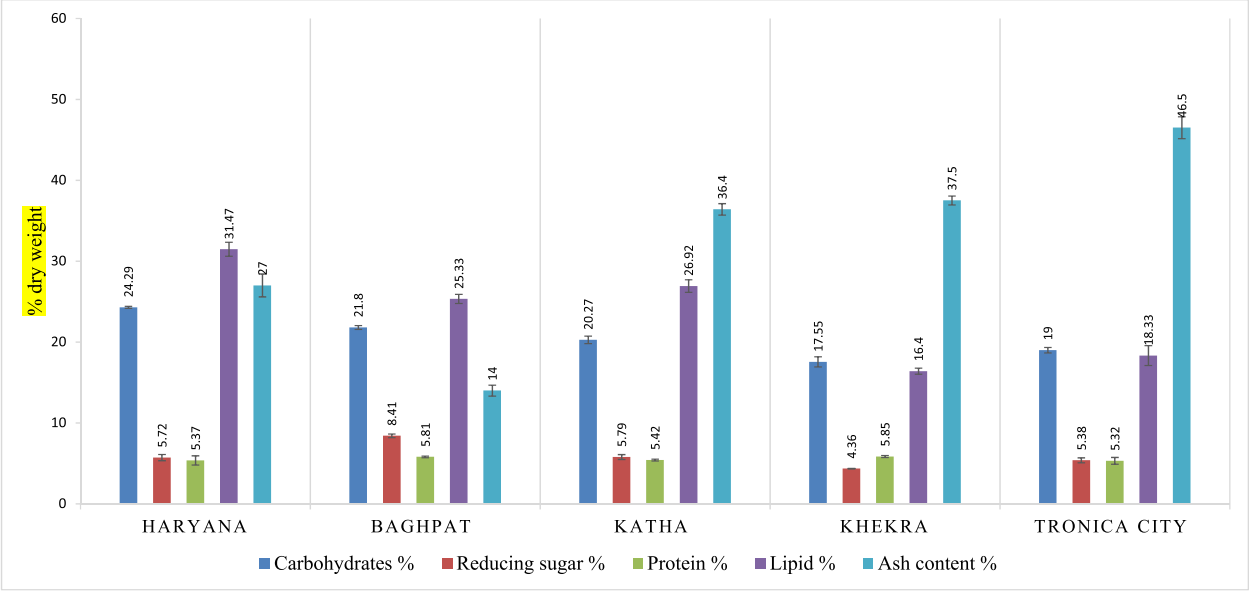


Fig. 1a. Percentage of Carbohydrates, Reducing Sugar, Protein, Lipid and Ash content in *Hydrodictyon* collected from different locations.

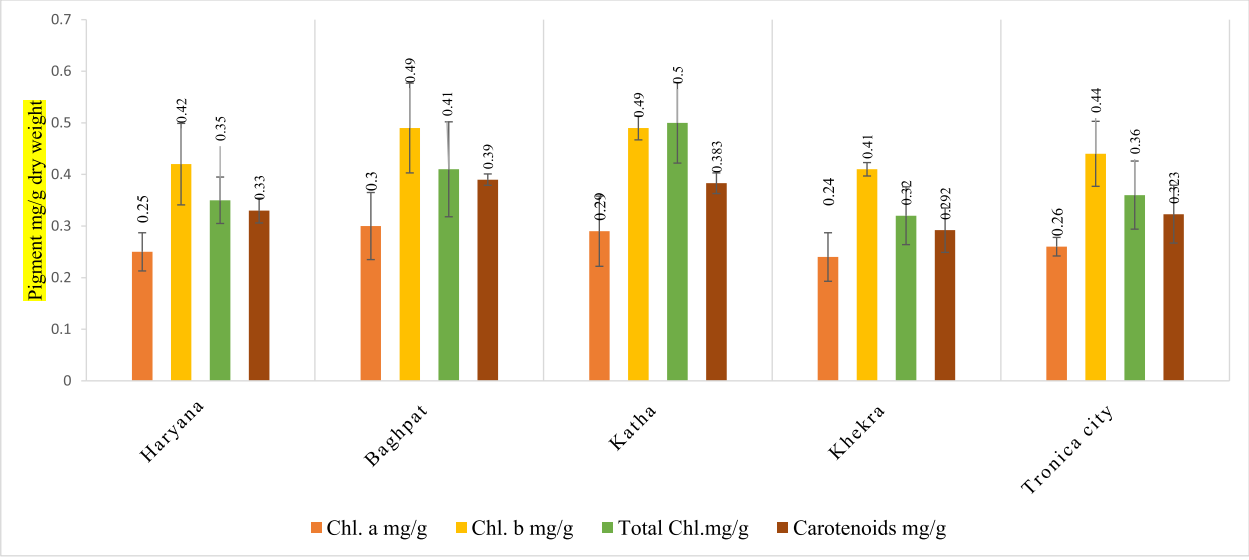


Fig. 1b. Concentration variation in Chl. a, Chl. b, Total Chl., and Carotenoids content in *Hydrodictyon* collected from different locations.

lipids such as N-ethyl N-(2-hydroxy-ethyl) arachidonoyl amine and the omega-3 derivative 2-Hydroxy-1-(hydroxymethyl)ethyl (6Z,9Z,12Z)-6,9,12-octadecatrienoate highlights potential signalling functions. Antioxidant and anti-inflammatory phenolics, including Salvianolic acid L, Diosmetin, Stigmasterol, Morin, and Malabaricone C, along with flavonoid glycosides like (+)-Myristinin A, Dihydromyricetin-3-O-xyl, and Dihydroquercetin-glucosyl-rhamnoside, suggest cytoprotective properties. Additionally, lesser-known compounds such as alpha- Carboxy Dimethyl Butyl Hydroxy Chroman and Pentaphlorethol contribute to the unique metabolic fingerprint of the extract.

3.3. CHNS analysis of hydrodictyon

CHNS analysis shows the content of Carbon, Hydrogen, Nitrogen, and Sulphur varied in each sample. Carbon 38.05 ± 0.50%, Hydrogen 5.18 ±0.57%, and Nitrogen 5.26 ±0.60% content was found maximum in the sample of Baghpat while sulphur content was found to be a maximum of 1.65 ±0.14% sample of Tronica city (Table 3, Fig. 3).

3.4. FTIR analysis

Fourier transform infrared (FTIR) analysis shows the presence of special compounds, Alcohol, Phenol, carboxylic acid, Alkane, aldehyde, Alkyne, Nitriles, Ketone, Aromatic compounds, Fluoride, Esters, Ether, Alcohol, Anhydride, Cyanide, Alkyl halide in the sample. As shown in (Table 4, Fig. 4).

3.5. Statistical analysis of metabolites and CHNS composition across locations

A one-way ANOVA was performed to assess variations in metabolite abundance in *Hydrodictyon* biomass collected from different geographic locations. The analysis revealed a statistically significant difference between groups ($F(17,72) = 1633.94$, $p < 0.0001$), indicating substantial location-based variability in metabolite profiles (Table 5a). Similarly, CHNS elemental composition also showed significant variation across sampling sites. One-way ANOVA for CHNS data yielded an F-

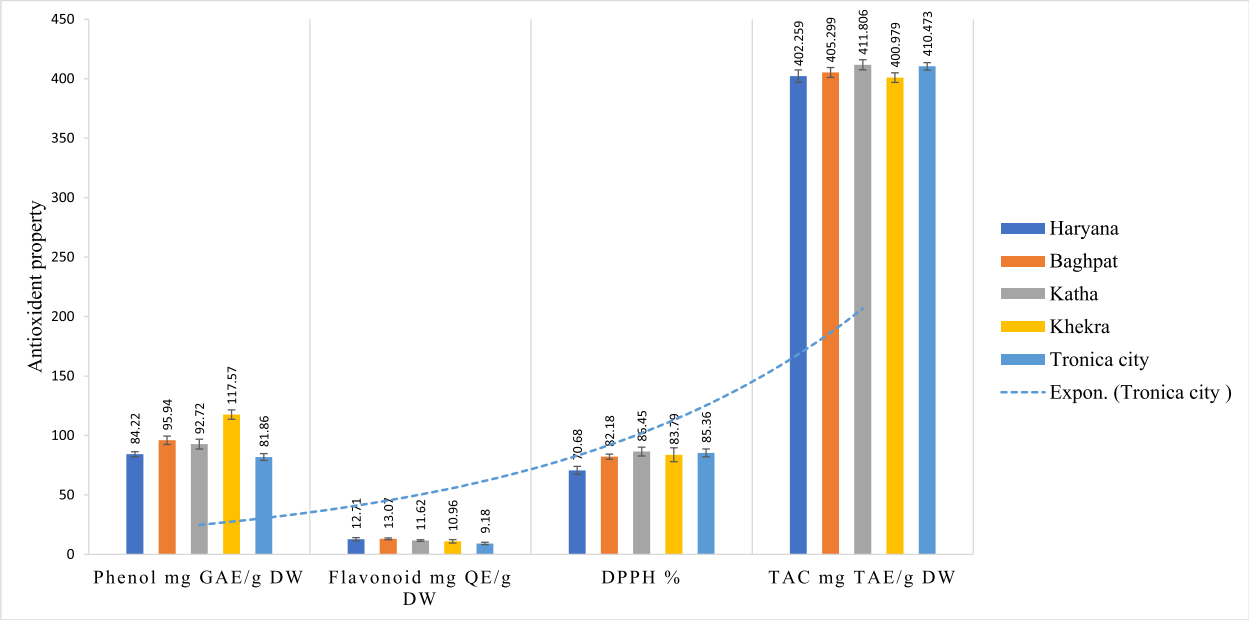


Fig. 1c. Concentration variation in Phenol, Flavonoids, DPPH, and TAC content in *Hydrodictyon* collected from different locations.

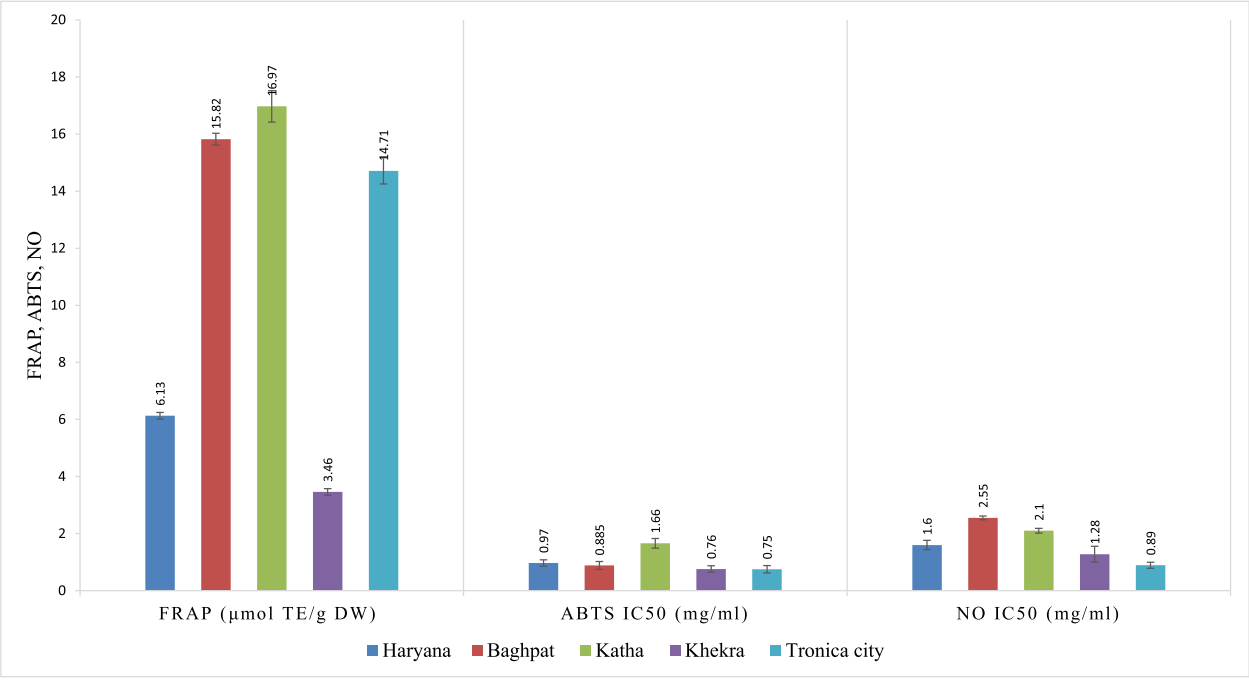


Fig. 1d. Variation in antioxidant capacity, FRAP, ABTS and NO concentration in *Hydrodictyon* collected from different locations.

value of 86.63 (F (5,24), $p < 0.0001$), confirming a strong influence of location on elemental composition (Table 5b).

4. Discussion

Pollution induced stress in algae disrupts photosynthesis and promotes oxidative imbalance, leading to a reduction in primary metabolites such as carbohydrates, proteins, and lipids. In contrast, the enhanced accumulation of secondary metabolites, particularly phenolics, flavonoids, and proline, reflects an adaptive defence strategy against environmental stressors. (Ramakrishnan et al., 2010). *Hydrodictyon* demonstrates remarkable metabolic plasticity when exposed to environmental stress. Variations in its bioactive compound profile across different sampling sites of the heavily polluted Yamuna River indicate physiological adaptations to pollution. This resilience underscores its potential as a promising source of antioxidant metabolites for nutritional, pharmaceutical, and biotechnological applications.

Lipid levels in *Hydrodictyon* were consistently higher than proteins and carbohydrates, positioning this species as a potential candidate for biodiesel production and fatty acid recovery (Fig. 1a). Reported lipid yields exceeded or were comparable to those from other microalgae cultivated in wastewater streams, such as *Monoraphidium obtusum, Ankistrodesmus falcatus*, and *Chlorella* sp. (Kumar et al., 2016; Sharma et al., 2020) . This suggests that pollution-stressed habitats may favour

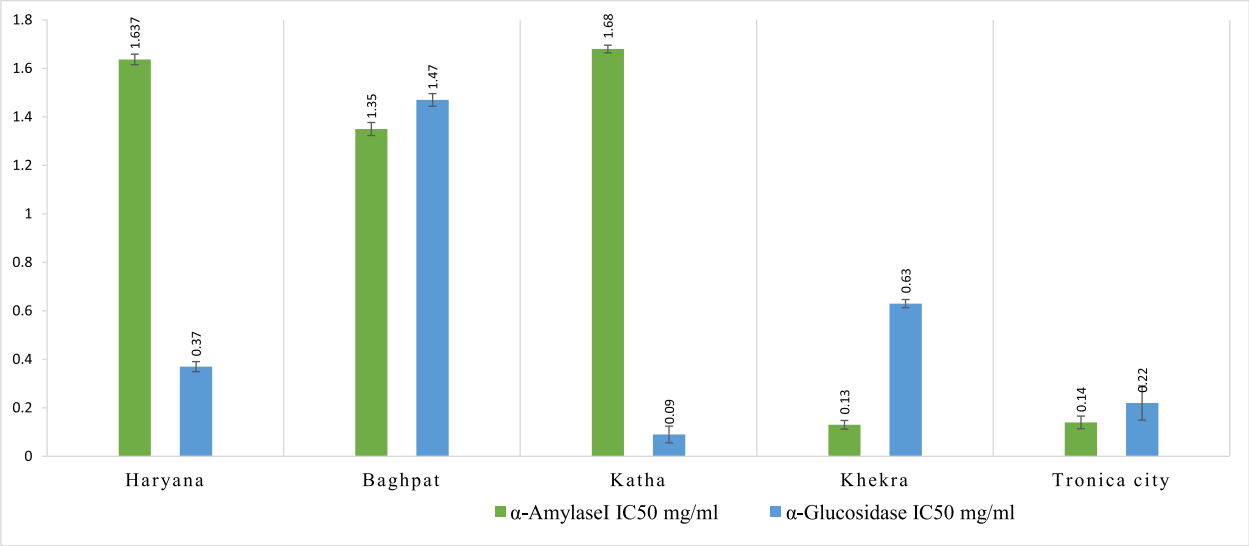


Fig. 1e. Variation in antidiabetic (α-amylase and α-glucosidase) activity in *Hydrodictyon* collected from different locations.

lipid accumulation, consistent with earlier reports that wastewater-grown microalgae often enhance lipid biosynthesis as a survival mechanism (de Alva et al., 2013; Qin et al., 2016).

Lipid content in *Hydrodictyon* varied significantly across sampling locations, with the highest accumulation observed in specimens from the Yamuna River at Haryana, followed by those from Katha and Baghpat. Conversely, samples from Khekra and Tronica City exhibited notably lower lipid levels (Fig. 1a). Across all locations, lipid levels in *Hydrodictyon* were consistently higher than those of proteins and carbohydrates, reinforcing its potential as a viable candidate for biodiesel production and fatty acid recovery (Fig. 1a). These lipid yields are comparable to or exceed those reported for other microalgae grown in wastewater environments, such as *Monoraphidium obtusum, Ankistrodesmus falcatus*, and *Chlorella* spp. (Kumar et al., 2016; Sharma et al., 2020). This trend supports earlier findings that pollution-stressed environments, such as wastewater-impacted water bodies, may favour lipid accumulation in microalgae. Previous studies have attributed this to a stress-induced survival mechanism, where microalgae enhance lipid biosynthesis under nutrient-limited or pollutant-rich conditions (de Alva et al., 2013; Qin et al., 2016). These variations in lipid metabolite profiles are not only important from a biofuel perspective but also carry significant implications for bioactivity. Environmental pollutants, including heavy metals and chemical contaminants, can disrupt lipid metabolism, leading to qualitative and quantitative changes in lipid composition. Such alterations may affect the concentration of key lipid classes like polyunsaturated fatty acids (PUFAs), which are associated with antimicrobial, anti-inflammatory, and antioxidant activities. A decrease in these beneficial lipids could compromise the organism's physiological defences and reduce its potential for pharmaceutical or nutraceutical applications. Conversely, stress conditions might also promote the production of novel lipid metabolites with enhanced or unique bioactivities (Nowicka, 2022). Therefore, the observed site-specific lipid variations in *Hydrodictyon* likely reflect localized environmental stress levels, highlighting a clear causal relationship between pollution, lipid metabolite profiles, and bioactivity. This underscores the importance of environmental context in evaluating the biotechnological and therapeutic potential of *Hydrodictyon*.

Although the carbohydrate and protein contents in *Hydrodictyon* were comparatively lower than lipid levels (Fig. 1a), their concentrations remained within the typical ranges reported for other green algal species (Becker, 2007; Uyaguari-Diaz et al., 2016). Notably, samples from Tronica City and Katha exhibited elevated ash content, indicating a substantial uptake of inorganic pollutants, including heavy metals (Fig. 1a). This suggests that *Hydrodictyon* is actively involved in the bioaccumulation of contaminants, reinforcing its role in the bioremediation of the Yamuna River ecosystem. However, this exposure to environmental pollution had clear metabolic consequences. The reduction in protein and carbohydrate levels in these samples' points to a stress-induced disruption of essential biosynthetic pathways. Carbohydrates and proteins are vital for energy storage and cellular structure, and their decline is likely linked to impaired photosynthetic activity and nutrient assimilation under pollutant stress (Nagappan et al., 2020). Heavy metals and other contaminants are known to generate oxidative stress, inhibit enzyme function, and interfere with nutrient uptake, leading to a metabolic shift that deprioritizes growth and structural maintenance in favour of survival. Similar responses have been observed in other freshwater algae, such as *Chlorella* sp., *Scenedesmus quadricauda*, and *Scenedesmus vacuolatus* (Gauthier et al., 2020), indicating a broadly conserved stress adaptation strategy.

Importantly, these pollution-induced metabolite variations have direct implications for bioactivity. Alterations in the quantity and composition of macromolecules such as lipids, proteins, and carbohydrates can influence the organism's functional properties, including antimicrobial, antioxidant, or anti-inflammatory effects. For instance, while lipid accumulation under stress may enhance certain bioactivities (e.g., through increased polyunsaturated fatty acids (Silva et al., 2025), a concurrent decline in proteins and carbohydrates may reduce nutritional or therapeutic value (El-Sheekh et al., 2023). Moreover, stress conditions may induce the synthesis of novel metabolites not present under normal conditions, potentially offering new bioactive compounds of interest. Thus, pollution not only shapes the metabolic profile of *Hydrodictyon* but also modulates its bioactive potential, underlining the importance of environmental context in evaluating its ecological role and biotechnological applications.

Pigment and phenolic analyses further emphasize the considerable antioxidant potential of *Hydrodictyon*, which appears closely linked to environmental conditions, particularly pollution stress. Concentrations of carotenoids, phenolics, and flavonoids in this species were frequently higher than those reported for other freshwater and marine microalgae (Hajimahmoodi et al., 2010; Safafar et al., 2015), underscoring its significant promise for nutraceutical applications (Fig. 1b). This increase in bioactive compounds is likely a direct response to pollution-induced oxidative stress, which triggers enhanced biosynthesis of secondary metabolites such as carotenoids and phenolics. These compounds serve as protective antioxidants, mitigating cellular damage from reactive oxygen species generated by contaminants. Correspondingly, extracts

Table 2
Qualitative analysis of secondary metabolites of methanolic extract of *Hydrodictyon thallus* by using LCMS.

Sr. No.	Compound	Category	Molecular weight g/mol	ESI^{+} m/z $[M + H]^{+1}$	Potential Nutraceutical Use	References
1	Pheophorbide-a	Chlorophyll derivative	592.7	593.30	Anticancer, antiviral (SARS-CoV-2, HCV), improves glucose uptake, anti-aging (skin), antioxidant	10.3389/fendo.2024.1330058; 10.7717/peerj.14568,
2	1-[11Z,14Z-eicosadienoyl]-2-dodecanoyl-glycero-3-phospho-[1′-sn-glycerol]	Phospholipid	718.9	719.45	Influences membrane dynamics and signaling; used in lipid and membrane biology research	10.1139/bcb-2015-0149
3	Enigmol	Terpenoid	301.5 g/mol	302.30	Antioxidant, potential neuroprotective effects, under study for roles in sphingolipid metabolism and cancer	10.1158/1535-7163.MCT-10-0754; 10.5530/ijper.58.4.141
4	2,5-Dichloro-4-oxohex-2-enedioate	Fatty acid	227.00	227.176	Mainly used in research (schizophrenia) no direct known health benefits; intermediate in chemical synthesis	10.1016/j.neubiorev.2019.04.010
5	Hexadecasphinganine	Sphingolipid	273.45	274.27	Precursor in sphingolipid biosynthesis; important for cell growth, apoptosis, and neural development	10.1016/j.jlr.2025.100813; 10.1016/j.bioorg.2007.10.002; 10.1016/j.clinbiochem.2010.04.072
6	Hexadecyl Acetyl Glycerol	Glycerolipid	358.6	359.31	Immune-modulating and antiviral potential; found in human milk and some immune cells, Omega-3 delivery, anti-inflammatory	10.1016/S0006-291X(84)80108-4; 10.3389/fonc.2021.730638; 10.1017/S0007114525000273
7	N-ethyl N-(2-hydroxy-ethyl) arachidonoyl amine	Fatty acid	375.6	376.34	Neuroprotective, anti-inflammatory	https://ontosight.ai/glossary/term/n-n-2-2-dihydroxy-ethyl-arachidonoyl-amine-compound–679db64738099fda3cfcdac0,
9	2-Hydroxy-1-(hydroxymethyl)ethyl (6Z,9Z,12Z)-6,9,12-octadecatrienoate	Fatty acid	352.5	353.26	Anti-inflammatory and cardiovascular protective potential; derivative of omega-3 fatty acids	10.1016/j.pharmthera.2017.10.016
11	alpha-Carboxydimethyloctylhydroxychroman	Phenolic	390.6	391.28	Potential Nutraceutical Use	10.1007/s13369-021-05858-3
13	Salvianolic acid L		718.6	719.45	Potential antioxidant and anti-inflammatory properties; may support cardiovascular health.	10.1186/1423-0127-18-30, 10.3389/fphar.2020.572373
14	Choline	Quaternary ammonium compound	103.10	104.10	Essential nutrient for brain function, liver health, and muscle control; may reduce dementia risk by up to 23% with moderate intake	10.1016/S0899-9007(00)00349-X; 10.2174/187152412800792689
15	12,13-DiHOME	Oxylipin	314.25	315.15	Potential role in metabolic regulation; further research needed to determine human health benefits.	10.1016/j.lfs.2021.120229; 10.1155/2024/2506586
16	Diosmetin	Flavonoid	300.06	301.14	Potential antioxidant and anti-inflammatory properties; may support cardiovascular health.	10.1016/j.phyplu.2021.100179; 10.3390/biomedicines10051076
17	Stigmasterol	Sterol	412.69	413.26	Potential anti-diabetic, anti-inflammatory, and neuroprotective effects; may support cardiovascular health .	10.3390/antiox11101912; 10.1016/B978-0-12-822923-1.00019-4
18	Morin	Flavonoid	301.29	302.30	Potential antioxidant and anti-inflammatory properties; may support cardiovascular and neurological health.	10.1016/j.bbagen.2006.03.026; 10.1016/j.prmcm.2023.100264
19	Malabaricone C (Diarylnonanoid)	Phenolic lipid	358.1812	359.31	Potential antioxidant and anti-inflammatory properties; may support metabolic health.	10.1016/j.freeradbiomed.2012.02.013
20	(+)-Myristinin A (Flavan)	polyphenol	548.2774	548.50	Limited information available; further research needed to determine human health benefits.	10.7324/JAPS.2024.179965; 10.1002/efd2.90
21	Pentaphlorethol	polyphenol	622	623.38	Limited information available; further research needed to determine human health benefits.	10.1177/1934578 × 22110940; 10.3390/antiox11061055
22	Dihydromyricetin-3-O-xyl	Flavonoid	452.0793	453.0871	Potential antioxidant and neuroprotective properties; may	10.1016/j.focha.2022.100084; 10.3389/fendo.2023.1216907

(*continued on next page*)

Table 2 (*continued*)

Sr. No.	Compound	Category	Molecular weight g/mol	ESI^{+} m/z $[M + H]^{+1}$	Potential Nutraceutical Use	References
					support liver health and treatment of diabetes	
23	Dihydroquercetin-glucosyl- rhamnoside	Flavonoid	613.1162	613.38	Potential antioxidant and anti-inflammatory properties; may support cardiovascular health.	10.1016/j.focha.2022.100084; 10.1371/journal.pone.0264987

Table 3
CHNS analysis of *H. reticulatum* collected from different locations.

Sites	C %	H %	N %	S %
Haryana	21.14 ± 0.572	3.321 ±0.873	2.79 ±0.303	1.298 ±0.026
Baghpat	38.05 ± 0.504	5.182 ±0.578	5.26 ±0.606	1.258 ±0.073
Katha	30.6 ± 0.173	3.989 ±0.424	4.11 ±0.467	0.748 ±0.075
Khekra	29.38 ± 0.226	4.348 ±0.221	4.3 ±0.528	0.917 ±0.077
Tronica city	31.99 ± 0.406	4.9 ± 0.65	5.05 ±0.235	1.654 ±0.143

from *Hydrodictyon* exhibited potent antioxidant activities across multiple assays, including DPPH, ABTS, nitric oxide (NO) scavenging, and FRAP with samples from highly polluted sites like Tronica City showing particularly elevated activity (Fig. 1c-d). The antioxidant capacity of these extracts was comparable to, or exceeded, that of other well-characterized algal species as well as plant species (Sharifi-Rad et al., 2022; Sharifi Rad et al., 2014). Researcher demonstrated that pollution not only influences metabolite profiles but can also enhance the bioactive potential of the alga (Lopes et al., 2024). Thus, pollution acts as a key environmental driver shaping metabolite variation, which in turn modulates the antioxidant and overall bioactivity of *Hydrodictyon*, increasing its potential value in pharmaceutical and nutraceutical industries. These findings support the hypothesis that pollution-induced stress stimulates the production of secondary metabolites with antioxidant properties. Exposure to metal or organic contaminants generates reactive oxygen species (ROS), which can damage cellular structures and impair enzymatic functions. In response, algae activate antioxidant defense systems, resulting in the accumulation of protective compounds. For instance, *Scenedesmus* sp. IITRIND2 exhibited elevated levels of cysteine and glutamate when exposed to arsenic, demonstrating their important role in ROS scavenging (Arora et al., 2018). This adaptive mechanism highlights the metabolic flexibility of algae under environmental stress and reinforces their potential as valuable sources of bioactive antioxidant compounds.

Notably, enzyme inhibition assays demonstrated significant α-amylase and α-glucosidase inhibitory activity in *Hydrodictyon* extracts, in some cases approaching the efficacy of the standard antidiabetic drug acarbose and plants extracts (Benmohamed et al., 2023) (Fig. 1e). These results highlight the potential of *Hydrodictyon* as a natural source for managing postprandial hyperglycemia and support its application in functional food formulations and nutraceuticals targeting diabetes management (Poovitha and Parani, 2016). Importantly, the observed bioactivities are closely tied to the metabolite profiles of the algae, which appear to be modulated by environmental stressors such as pollution. Pollution, particularly from heavy metals and organic contaminants, is known to induce oxidative stress in aquatic organisms, prompting a metabolic shift toward the biosynthesis of defensive and protective secondary metabolites (Kumar et al., 2025). This adaptive response was evident in the metabolomic profiling of *Hydrodictyon*, which revealed a diverse array of bioactive compounds with therapeutic relevance, including pheophorbide-a, a tetrapyrrole with anticancer, antiviral, photodynamic, anti-inflammatory, and antioxidant properties; Enigmol, a tumor-suppressive sphingolipid analog that also modulates apoptosis and cell proliferation; and bioactive phospholipids, flavonoids, sterols, and oxylipins involved in membrane stabilization, anti-inflammatory signaling, and lipid metabolism (Symolon et al., 2011). Pheophorbide-a from marine algae improves postprandial hyperglycemia through dual actions on carbohydrate-digesting enzymes and pancreatic insulin secretion, functioning as an insulin-mimetic agent, digestive enzyme inhibitor, and modulator of oxidative stress pathways (Lee et al., 2021). Malabaricone C, a natural sphingomyelin synthase inhibitor, enhances glucose tolerance in high-fat diet mice while mitigating oxidative and nitrosative stress–mediated gastric injury, and exhibits anti-inflammatory, hepatoprotective, and neuroprotective effects, linking membrane lipid remodeling to antioxidant, antidiabetic, and cytoprotective functions (Othman et al., 2019; Basak et al., 2020). Flavonoids such as Morin simultaneously lower blood glucose, enhance insulin signaling, protect retinal tissue, and exert anti-inflammatory, cardioprotective, and neuroprotective effects via modulation of oxidative stress, inflammation, and carbohydrate-metabolizing enzymes (Vanitha et al., 2014: Kumar et al., 2026). Similarly, diosmetin improves hyperglycemia by upregulating the IRS/PI3K/AKT pathway, modulating gut microbiota, and providing anti-inflammatory, hepatoprotective, and lipid-lowering effects, highlighting its multi-target antioxidant, antidiabetic, and metabolic regulatory profile (Gong et al., 2021). Dihydromyricetin exhibits strong free radical scavenging, activates Nrf2/HO-1 antioxidant defenses, and improves obesity- and diabetes-related metabolic disturbances while providing hepatoprotective and neuroprotective benefits, integrating redox regulation with energy metabolism (Liu et al., 2019). Glycosylation patterns, such as rhamnosyl glucoside conjugation in quercetin derivatives, enhance iron-chelating antioxidant activity, stabilize flavonoid structures, improve bioavailability, and confer cardioprotective, anti-inflammatory, and antidiabetic effects, exemplified by dihydroquercetin glucosyl rhamnoside (Omololu et al., 2011). Collectively, these metabolites demonstrate multifunctional therapeutic potential, including antioxidant, antidiabetic, neuroprotective, immunomodulatory, cardioprotective, hepatoprotective, and anti-inflammatory activities, highlighting the value of *Hydrodictyon* as a source of biofunctional compounds for drug discovery and nutraceutical applications (Fig. 2). Many of these metabolites also possess neuroprotective, immunomodulatory, and cardioprotective properties (Stonik & Stonik, 2018). Notably, elevated levels of such compounds, particularly in samples from more polluted environments, underscore the role of environmental stress in driving metabolic reprogramming. Consequently, pollution-induced variations in metabolite profiles not only alter the biochemical composition of *Hydrodictyon* but may also enhance or diversify its bioactive potential, reinforcing its value as a source of therapeutic agents and biofunctional compounds for drug discovery and nutraceutical applications.

Elemental (CHNS) and FTIR analyses revealed clear spatial variation in functional group composition and pollutant uptake across sampling sites, highlighting the environmental sensitivity of *Hydrodictyon*. Notably, sulfur enrichment observed in samples from Tronica City suggests significant industrial contamination, likely from sulfur-containing compounds commonly found in effluents from chemical and manufacturing sectors (Fig. 3, 4). In addition, the detection of pollutant-derived functional groups such as alkyl halides and cyanides further supports the presence of anthropogenic inputs. These compounds are typically associated with industrial waste and are known to interfere with cellular metabolism in aquatic organisms (Huang et al., 2015). Their accumulation in algal biomass not only underscores the

Table 4
FT-IR Transmission frequencies (cm^{-1}), functional group, and compounds of *H. reticulatum* collected from different locations.

Wave number (cm^{-1})	Assigned Group(s)	Metabolites	Biological Significance
3300–3500	O–H stretch (Alcohol, Phenol, Carboxylic Acid)	Phenolic compounds (flavonoids, tannins), Hydroxy acids	Antioxidant, anti-inflammatory
3400	Broad O–H stretch (Alcohol, Phenol)	Gallic acid, Quercetin, Catechins	Antioxidant, ROS scavenging, anti-inflammatory
3200–3500	Alcohol, phenol, carboxylic acid	Quercetin, gallic acid, caffeic acid	Antioxidant, anti-inflammatory
2850–2950	C–H stretch (Alkanes, Aldehydes)	Fatty acids, Steroids, Lipid metabolites	Structural components, membrane integrity
2850–2950	C–H stretch (Alkane, Aldehyde)	Fatty acids (e.g., Palmitic acid), Sterols	Membrane integrity, signalling lipids
2800–3000	Alkane, aldehyde	Fatty acids, sterols, aldehydes	Membrane components, signalling
1700–1750	C=O stretch (Ketones, Aldehydes, Carboxylic Acids, Esters)	Organic acids (citric acid, lactic acid), Esters of plant volatiles	Metabolic intermediates, energy metabolism
1700–1740	C=O stretch (Carboxylic acid, Ester)	Ferulic acid, Caffeic acid, Lactic acid, Citric acid	Energy metabolism intermediates, cytoprotection
1700	Ketone, carboxylic acid	Ferulic acid, caffeic acid, citric acid	Energy metabolism, cytoprotection
1600–1650	C=C or C=O stretch (Aromatics, Amides)	Aromatic rings in polyphenols, Proteins (Amide I)	Structural and enzymatic activity
1600–1650	C=C stretch (Aromatic), N–O (Nitro)	Flavonoids, Phenolic acids, Nitro-derivatives	Antioxidant, antimicrobial
1400–1600	Nitro, aromatic	Nitroaromatic compounds	Potential stress markers
1450–1500	C–H bending (Alkanes), N–O (Nitro)	Lipid-related compounds, Nitrogenous metabolites	Lipid signalling, possible nitrosative stress indicators
1250–1300	C–O stretching (Esters, Ethers)	Terpenoids, Essential oil esters, Lignins	Antimicrobial, membrane disruption
1200–1300	Nitro, alkane, fluoride	Nitro compounds, alkanes, fluorides	Possible signalling or contamination
1050–1300	C–O stretching (Alcohols, Esters, Ethers)	Sugars (glucose, fructose), Esters of terpenoids	Energy supply, flavour/aroma compounds
1000–1150	C–O–C, C–O stretch (Sugars, Alcohols)	Glucose, Fructose, Polyols	Energy source, Osmo protectant
900–1100	Cyanide, esters, ether	Cyanogenic compounds, esters	Defence compounds
700–900	Esters, ether	Esters, ethers	Flavour, aroma, antimicrobial
500–1000	C–X (Halides), Out-of-plane bends (Aromatic, Alkene)	Less common metabolites or synthetic contaminants	Often ignored unless confirmed
500–800	C–X stretch (Halides), aromatic out-of-plane	Possibly minor halogenated compounds or structural motifs	Minor bioactivity, contamination indicator
400–600	Alkyl halide	Alkyl halides	Possibly contaminants or synthetic residues

vulnerability of *Hydrodictyon* to environmental pollution but also highlights its utility as a bioindicator for monitoring aquatic ecosystem health. This capacity for pollutant uptake and associated metabolic responses strengthens the case for *Hydrodictyon* as both a biomonitoring agent and a model organism for studying stress-induced biochemical adaptations in freshwater systems. Collectively, these findings demonstrate that *Hydrodictyon* responds to pollution-induced stress through dynamic alterations in its metabolome, leading to the accumulation of a diverse array of bioactive compounds with significant biotechnological potential. This adaptive capacity underscores its dual functional role as both a producer of high-value nutraceutical metabolites and an effective bioremediator in polluted aquatic environments. The ability to simultaneously detoxify water bodies while generating compounds of pharmaceutical, nutritional, and industrial relevance highlights the ecological and commercial importance of this species. Future research should prioritize the targeted isolation and structural characterization of key metabolites, in vivo validation of their bioactivities, and the development of integrated, sustainable biorefinery models incorporating *Hydrodictyon* as a multifunctional biomass resource.

The FTIR spectrum reveals absorption bands corresponding to multiple functional groups, which, when rigorously matched to known metabolomic profiles, provide a deeper and more insightful understanding of the bioactive compounds present and their biological relevance (Tessaro et al., 2023). While FTIR analyses often remain generic merely assigning broad functional groups without connecting them to specific metabolites or their biological significance this integrated approach bridges that gap, offering mechanistic insight into the metabolome. For instance, the broad and intense band observed between ~3300 and 3500 cm^{-1} corresponds primarily to O–H stretching vibrations from hydroxyl groups found in phenolic compounds such as quercetin, gallic acid, and catechins key antioxidants identified in metabolomic studies. The hydrogen bonding inherent in these polyphenols not only broadens this peak but also reflects their biological function as reactive oxygen species (ROS) scavengers, underpinning their anti-inflammatory and cytoprotective roles (Kassem et al., 2023).

Absorptions in the 2850–3000 cm^{-1} region arise from C–H stretching of alkanes and aldehydes, which match well with fatty acids (e.g., palmitic acid) and sterols found via metabolomic analysis. These lipid metabolites are vital for maintaining cellular membrane integrity and engaging in signalling pathways, illustrating how FTIR spectral data correlate with critical biological functions (Grace et al., 2020).

Strong bands around 1700–1750 cm^{-1} are attributable to carbonyl (C=O) stretching vibrations from organic acids such as citric acid, lactic acid, ferulic acid, and caffeic acid, metabolites detected in metabolomic assays that act as intermediates in energy metabolism (Krebs cycle) and exhibit cytoprotective effects. This direct link between spectral features and metabolic pathways enhances the biological relevance of the FTIR data. The region near 1600–1650 cm^{-1} encompasses C=C and C=O stretches from aromatic rings in polyphenols and amide bonds in proteins, matching flavonoids and phenolic acids identified by metabolomics. The detection of nitro (N–O) groups here further suggests nitro-derivatives with known antimicrobial activity, aligning with the sample's observed bioactivity.

Bands around ~1400–1500 cm^{-1} correspond to C–H bending in alkanes and N–O vibrations in nitrogenous metabolites, indicating lipid signalling molecules or markers of nitrosative stress. These features provide clues to inflammatory and stress-response pathways reflected in the metabolomic profile. Vibrations in the ~1250–1300 cm^{-1} and ~1050–1300 cm^{-1} ranges arise from C–O stretching of esters, ethers, alcohols, terpenoids, essential oil esters, lignins, and sugars (glucose, fructose) all confirmed through metabolomic analysis. These metabolites contribute to energy storage, osmoprotection, and sensory

Table 5a
One way ANOVA analysis of metabolites in *Hydrodictyon* biomass collected from different Locations.

ANOVA *Source of Variation*	*SS*	*df*	*MS*	*F*	*P-value*	*F crit*
Between Groups	781781.53	17	45987.14894	1633.937633	5.328E-86	1.766576677
Within Groups	2026.4389	72	28.14498424			
Total	783807.97	89				

Table 5b
One-way ANOVA analysis of CHNS in *Hydrodictyon* biomass collected from different Locations.

ANOVA *Source of Variation*	*SS*	*df*	*MS*	*F*	*P-value*	*F crit*
Between Groups	2816.811	5	563.3621444	86.62704767	1.47616E-14	2.620654148
Within Groups	156.0793	24	6.503305371			
Total	2972.89	29				

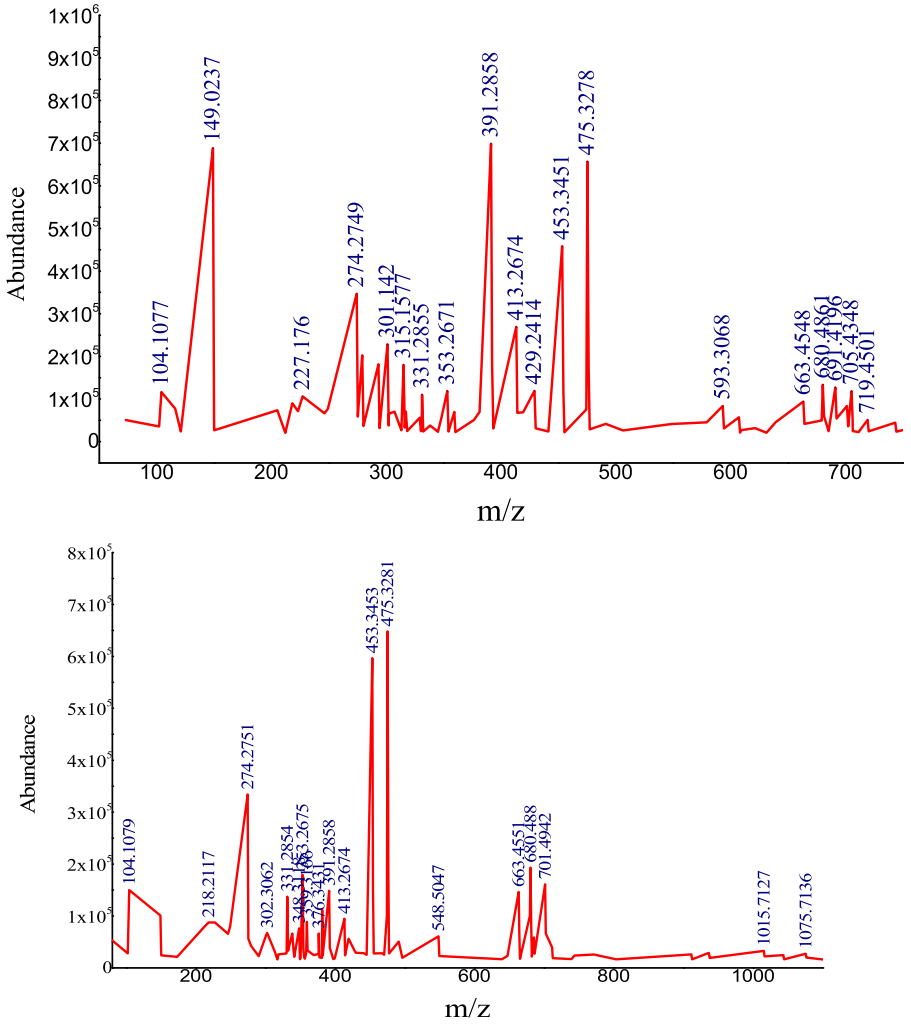


Fig. 2. LC-MS/MS spectrum showing peaks corresponding to the presence of various metabolic compounds.

properties like flavour and aroma. Peaks between 900–1100 cm^{-1} indicate cyanogenic compounds and esters, known plant defense molecules identified in metabolomics that protect against herbivores and pathogens. Signals in the 500–1000 cm^{-1} range correspond to C–X (halide) stretches and out-of-plane bending in aromatic or alkene groups, potentially revealing minor halogenated metabolites or environmental contaminants, emphasizing the need for careful interpretation.

Finally, weak bands at 400–600 cm^{-1} suggest alkyl halides, which, though generally minor and less biologically active, inform on sample purity or environmental exposure. By correlating FTIR absorption bands with specific metabolites and their known biological activities from metabolomic data, this analysis transcends generic spectral assignments. It provides mechanistic insight into the biochemical complexity of the sample, elucidating how functional groups correspond to key bioactive compounds and their roles in antioxidant defence, metabolism, signalling, and plant defence mechanisms.

Principal component analysis (PCA) is used to identify the correlation and variance found in the data set. It is a well-known multivariate

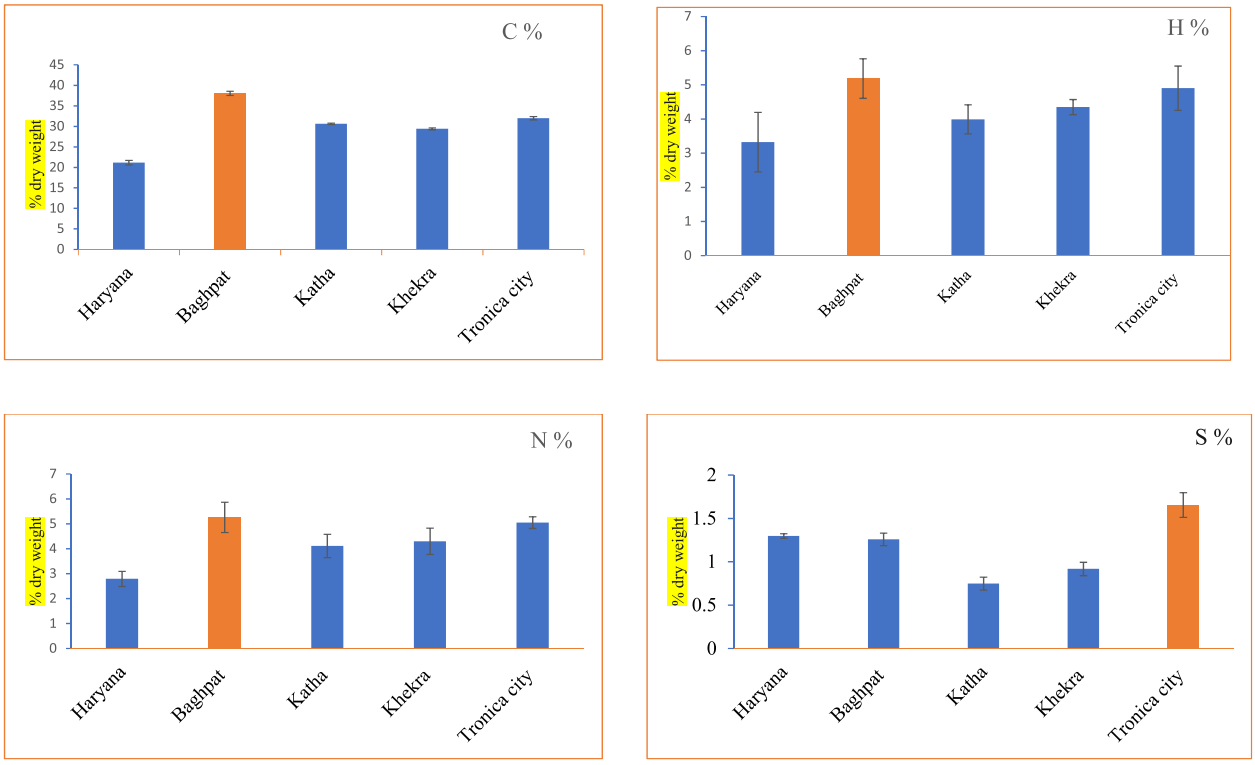


Fig. 3. CHNS analysis of *Hydrodictyon* biomass Collected from different locations.

method that converts many correlated variables into multiple non-linearly correlated variables known as principal components. In applications, PCA is applied to convert a high dimensional data set to a lower dimensional dataset, using only the first few principal components to reduce the size of the transformed data (Mahmoudi et al., 2021). The score plot of metabolites shows the maximum variance found in TAC, Phenol and α-glucosidase while other compounds are strongly correlated to each other, when one changes, the other will also change (Fig. 5a), while the biplot of PCA) shows that correlation exists among metabolite concentrations found in the biomass of Haryana, Katha, and Tronica City. Maximum variance has been shown by biomass collected from the Khekra site, followed by Baghpat. The biplot shows the distribution of metabolites along with collection sites, and it was found that phenol and DPPH content were found at their maximum at the Khekra site, while TAC was found at its maximum at sites in Haryana, Katha, and Tronica City. The maximum variance of metabolites is shown by the biomass collected from Khekra (Fig. 5b).

Hierarchical clustering analysis of metabolites shows similarity shown by carbohydrates and α-amylase with lipids while Chl. a shows similarity with Chl. b, Total chlorophyll, carotenoid, and α-glucosidase and phenol with protein. Reducing sugar is similar to Flavonoids while DPPH is similar to phenol. TAC is a single group and acts as an outgroup. Hierarchical clustering analysis shows DPPH is directly correlated to phenol and plays an important role in antioxidant activity (Fig. 5c).

Box plot analysis reveals that all the metabolites found in biomass collected from different locations have a nearly equal distribution of metabolites except for one of two outliers, while more distributed data are found in biomass collected from Katha and Haryana (Fig. 5d). One-factor ANOVA was used for the analysis, and it demonstrates the significant level of variation found in metabolites in samples collected from various locations. Rows represent metabolites, while columns represent collection sites, and F- value (1633.937633) > F crit (1.766576677) and P value (5.328E-86) < 0.05 is significantly less than the alpha value. The results show significant variation in metabolites collected from various locations and data is statically significant (Table 5a).

A significant level of variation and data significance is revealed by a one-way ANOVA analysis of CHNS concentrations. Because F-value (86.62704767) is greater than the F-crit value (2.620654148) and the P value (1.47616E-14) is less than 0.05, the data is statistically significant (Table 5b).

5. Conclusion and future perspectives

- This study presents the first comprehensive metabolite profiling of *H. reticulatum* collected from Yamuna River water, demonstrating its significant biochemical diversity.
- The algal biomass was found to be rich in phenolics, flavonoids, pigments, and lipids, indicating strong potential as a nutraceutical resource.
- High levels of bioactive compounds contributed to notable antioxidant and free-radical scavenging activities, supporting its potential use in health-promoting formulations.
- The presence of metabolites associated with anti-diabetic activity suggests possible applications in functional foods and therapeutic research.
- Variations in metabolite composition across different sampling sites highlight the influence of environmental conditions on biochemical profiles.
- The lipid content and overall biomass productivity indicate that *H. reticulatum* could serve as a promising feedstock for biofuel production.

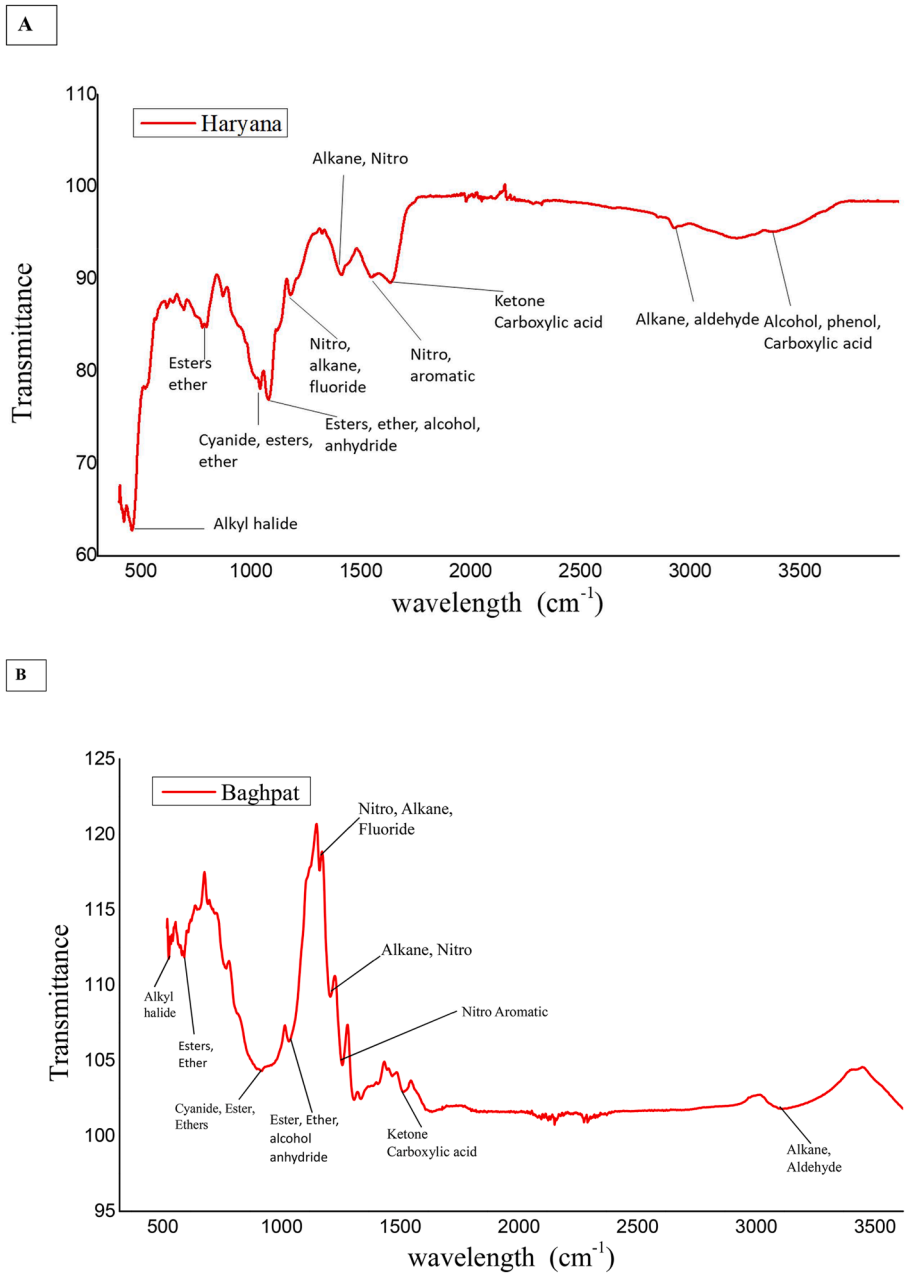


Fig. 4. FTIR analysis of *Hydrodictyon* biomass collected from different locations (A. Haryana, B. Baghpat, C. Katha, D. Khekra, and E. Tronica City) shown the presence of various functional groups.

- The species also demonstrates potential for phycoremediation, reinforcing its value in environmental sustainability and wastewater management.

Further work is needed for detailed biochemical and molecular characterization of individual bioactive compounds. *In vivo* studies should be conducted to validate the pharmacological and nutraceutical efficacy of the identified metabolites. Comprehensive toxicity and safety assessments are essential before considering food or pharmaceutical applications. Optimization of cultivation and large-scale production strategies will be critical to enable commercial exploitation.

Consent to participate

"Not applicable".

Consent for publication

"Not applicable".

Ethical statements

Human and animal rights

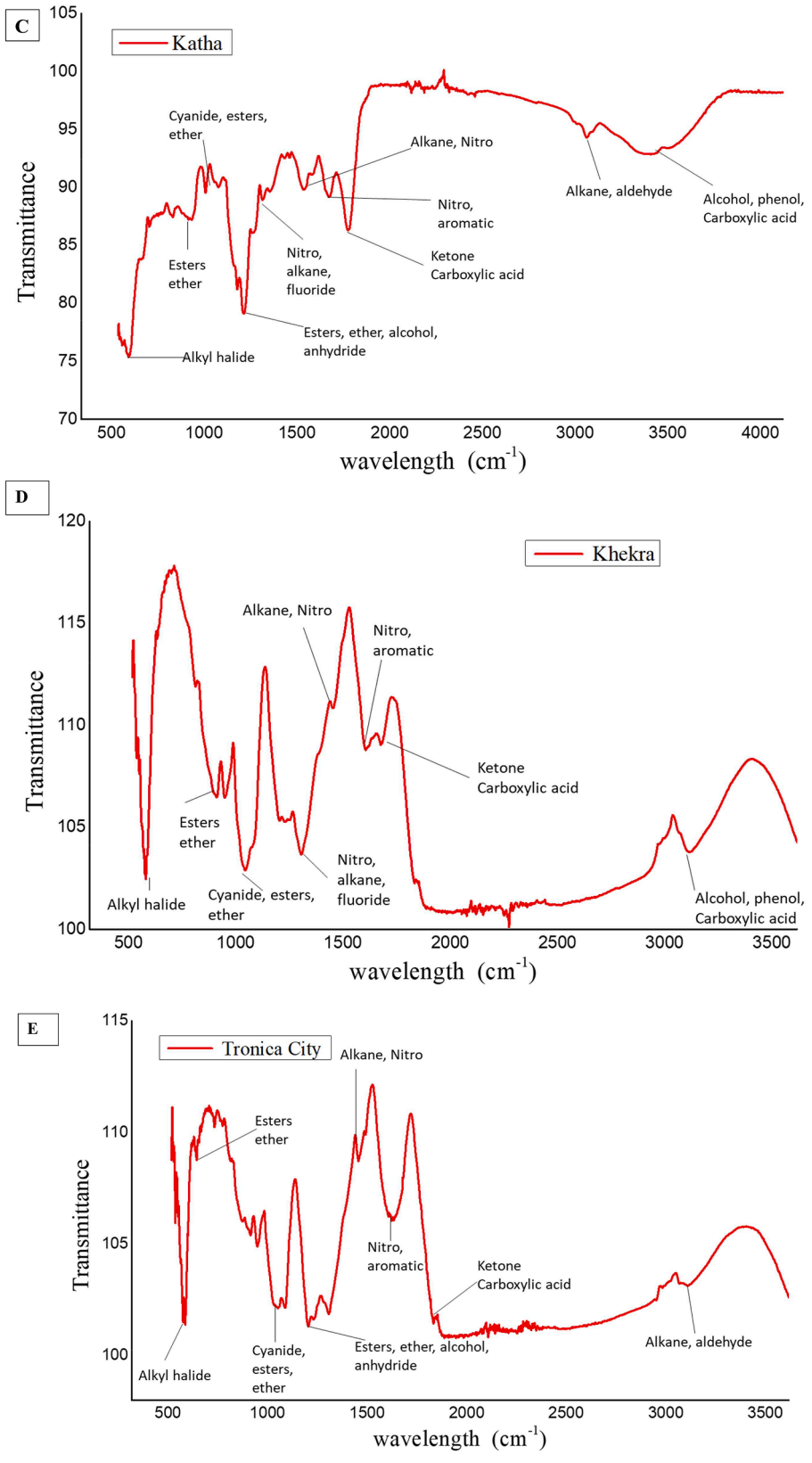


Fig. 4. (*continued*).

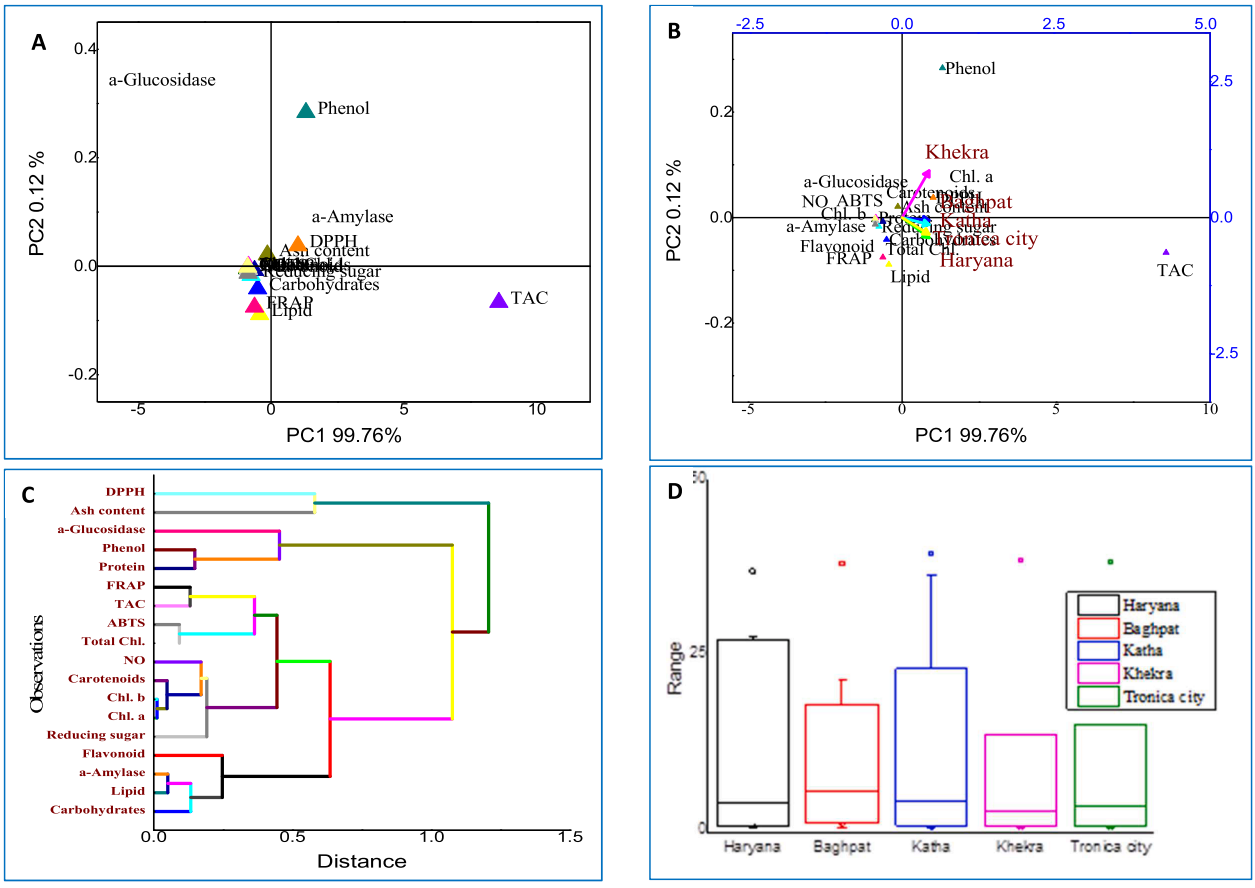


Fig. 5. PCA analysis of Metabolites **(A).** Score plot **(B).** Biplot **(C).** Box plot **(D).** AHC.

The authors declare that the work described has not involved experimentation on humans or animals.

Informed consent and patient details

The authors declare that the work described does not involve patients or volunteers.

Funding

This work did not receive any grant from funding agencies in the public, commercial, or not-for-profit sectors.

CRediT authorship contribution statement

Dharmendra kumar: Writing – original draft, Software, Resources, Methodology, Investigation, Data curation. **Shivankar Agrawal:** Writing – review & editing, Validation, Supervision, Formal analysis. **Manisha Prajapati:** Software, Resources. **Sanjukta Sahoo:** Project administration. **Dinabandhu Sahoo:** Supervision, Project administration, Funding acquisition, Conceptualization.

Declaration of competing interest

The authors declare that they have no known competing financial interests or personal relationships that could have appeared to influence the work reported in this paper.

Data availability

No data was used for the research described in the article.

References

Abo-Shady, A. M., Gheda, S. F., Ismail, G. A., Cotas, J., Pereira, L., & OH, Abdel-Karim (2023). Antioxidant and antidiabetic activity of algae. *Life, 13*(2), 460.

Agrawal, S., Barrow, C. J., Adholeya, A., & Deshmukh, S. K. (2022). Unveiling the dermatological potential of marine fungal species components: Antioxidant and inhibitory capacities over tyrosinase. *Biotechnology and Applied Biochemistry, 69*(3), 1252–1266.

Anjali, K., Sangeetha, B., Devi, G., Raghunathan, R., & Dutta, S. (2019). Bioprospecting of seaweeds (Ulva lactuca and Stoechospermum marginatum): The compound characterization and functional applications in medicine-a comparative study. *Journal of Photochemistry and Photobiology B: Biology, 200*, Article 111622.

Arora, N., Dubey, D., Sharma, M., Patel, A., Guleria, A., Pruthi, P. A., Kumar, D., Pruthi, V., & Poluri, K. M. (2018). NMR-based metabolomic approach to elucidate the differential cellular responses during mitigation of arsenic (III, V) in a green microalga. *ACS Omega, 3*(9), 11847–11856.

Association of Official Analytical Chemists. (2000). *Official methods of analysis of the Association of Official Analytical Chemists, 11*. The Association.

Barsanti, L., & Gualtieri, P. (2022). *Algae: Anatomy, Biochemistry, and Biotechnology*. CRC press.

Basak, M., Mahata, T., Chakraborti, S., Kumar, P., Bhattacharya, B., Bandyopadhyay, S. K., … Maity, B. (2020). Malabaricone C attenuates nonsteroidal anti-inflammatory drug-induced gastric ulceration by decreasing oxidative/nitrative stress and inflammation and promoting angiogenic autohealing. *Antioxidants & Redox Signaling, 32*(11), 766–784.

Becker, E. W. (2007). Micro-algae as a source of protein. *Biotechnology Advances, 25*(2), 207–210.

Becker, E. W. (2013). Microalgae for human and animal nutrition. *Handbook of Microalgal Culture: Applied Phycology and Biotechnology*, 461–503.

Benmohamed, M., Guenane, H., Messaoudi, M., Zahnit, W., Egbuna, C., Sharifi-Rad, M., Chouh, A., Seghir, B. B., Rebiai, A., & Boubekeur, S. (2023). Mineral profile, antioxidant, anti-inflammatory, antibacterial, anti-urease and anti-α-amylase activities of the unripe fruit extracts of Pistacia atlantica. *Molecules, 28*(1), 349.

Bradford, M. M. (1976). A rapid and sensitive method for the quantitation of microgram quantities of protein utilizing the principle of protein-dye binding. *Analytical Biochemistry, 72*(1-2), 248–254.

Bürck, M., Nakamoto, M. M., Trindade, L. G., Souto, R. N. B., Tanaka, B. K. F., de Souza, I. F., & Braga, A. R. C. (2025). *Microalgae as a Source of Bioactive Compounds Bioactive Compounds* (pp. 28–44). CRC Press.

de Alva, M. S., VM, Luna-Pabello, Cadena, E., & Ortíz, E. (2013). Green microalga Scenedesmus acutus grown on municipal wastewater to couple nutrient removal with lipid accumulation for biodiesel production. *Bioresource Technology, 146*, 744–748.

DuBois, M., Gilles, K. A., Hamilton, J. K., Pt, Rebers, & Smith, F. (1956). Colorimetric method for determination of sugars and related substances. *Analytical Chemistry, 28*(3), 350–356.

El-Sheekh, M. M., Galal, H. R., Mousa, A. S. H., & Farghl, A. A. (2023). Coupling wastewater treatment, biomass, lipids, and biodiesel production of some green microalgae. *Environmental Science and Pollution Research, 30*(12), 35492–35504.

Fabrowska, J., Messyasz, B., Szyling, J., Walkowiak, J., & Łęska, B. (2018). Isolation of chlorophylls and carotenoids from freshwater algae using different extraction methods. *Phycological Research, 66*(1), 52–57.

Firuzi, O., Lacanna, A., Petrucci, R., Marrosu, G., & Saso, L. (2005). Evaluation of the antioxidant activity of flavonoids by "ferric reducing antioxidant power" assay and cyclic voltammetry. *Biochimica et Biophysica Acta (BBA)-General Subjects, 1721*(1-3), 174–184.

Gauthier, L., Tison-Rosebery, J., Morin, S., & Mazzella, N. (2020). Metabolome response to anthropogenic contamination on microalgae: a review. *Metabolomics, 16*(1), 8.

Gong, X., Xiong, L., Bi, C., & Zhang, B. (2021). Diosmetin ameliorate type 2 diabetic mellitus by up-regulating Corynebacterium glutamicum to regulate IRS/PI3K/AKT-mediated glucose metabolism disorder in KK-Ay mice. *Phytomedicine, 87*, 153582.

Grace, C. E. E., Lakshmi, P. K., Meenakshi, S., Vaidyanathan, S., Srisudha, S., & Mary, M. B. (2020). Biomolecular transitions and lipid accumulation in green microalgae monitored by FTIR and Raman analysis. *Spectrochimica Acta Part A: Molecular and Biomolecular Spectroscopy, 224*, Article 117382.

Guil-Guerrero, J. L., & Prates, J. A. (2025). Microalgae Bioactives for Functional Food Innovation and Health Promotion. *Foods, 14*(12), 2122.

Guiry, M. D., Guiry, G. M., Morrison, L., Rindi, F., Miranda, S. V., Mathieson, A. C., Parker, B. C., Langangen, A., John, D. M., & Bárbara, I. (2014). AlgaeBase: an on-line resource for algae. *Cryptogamie, Algologie, 35*(2), 105–115.

Gutierrez, R. M. P., Anaya Sosa, I., Cruz y Victoria, T., & Flores, J. M. M. (2012). Sesquiterpene lactones: antispasmodic principles of the freshwater algae Hydrodictyon reticulatum. *Medicinal Chemistry Research, 21*(7), 1023–1029.

Hajimahmoodi, M., Faramarzi, M. A., Mohammadi, N., Soltani, N., Oveisi, M. R., & Nafissi-Varcheh, N. (2010). Evaluation of antioxidant properties and total phenolic contents of some strains of microalgae. *Journal of Applied Phycology, 22*(1), 43–50.

Huang, J., Huang, Y., Pontius, R. G., Jr, & Zhang, Z. (2015). Geographically weighted regression to measure spatial variations in correlations between water pollution versus land use in a coastal watershed. *Ocean Coast Manage, 103*, 14–24.

International, A. (1996). AOAC international official methods of analysis. *AOAC International Gaithersburg*.

Jagetia, G. C., Rao, S. K., Baliga, M. S., & Babu K, S. (2004). The evaluation of nitric oxide scavenging activity of certain herbal formulations in vitro: a preliminary study. *Phytotherapy Research: An International Journal Devoted to Pharmacological and Toxicological Evaluation of Natural Product Derivatives, 18*(7), 561–565.

Kassem, A., Abbas, L., Coutinho, O., Opara, S., Najaf, H., Kasperek, D., Pokhrel, K., Li, X., & Tiquia-Arashiro, S. (2023). Applications of Fourier Transform-Infrared spectroscopy in microbial cell biology and environmental microbiology: advances, challenges, and future perspectives. *Frontiers in microbiology, 14*, Article 1304081.

Kumar, D., Agrawal, S., Kumar, M., & Sahoo, D. (2023). Assessment of nutritional constituents content and biomedical aspects of five Gracilaria species: a multivariate analysis. *Journal of Aquatic Food Product Technology*, 1–15.

Kumar, D., Agrawal, S., Sahoo, S., Geetanjali, E., & Sahoo, D. (2025). Metabolic plasticity and abiotic stress adaptation in freshwater algae during phycoremediation of polluted river water. *Plant-Environment Interactions, 6*(5), e70093.

Kumar, J., Dhar, P., Tayade, A. B., Gupta, D., Chaurasia, O. P., Upreti, D. K., Toppo, K., Arora, R., Suseela, M., & Srivastava, R. B. (2015). Chemical composition and biological activities of trans-Himalayan alga Spirogyra porticalis (Muell.) Cleve. *PLoS One, 10*(2), Article e0118255.

Kumar, K. S., Prasanthkumar, S., & Ray, J. (2016). Experimental assessment of productivity, oil-yield and oil-profile of eight different common freshwater-blooming green algae of Kerala. *Biocatalysis and Agricultural Biotechnology, 8*, 270–277.

Kumar, S., Raghuvanshi, A., Kumar, A., & Monga, V. (2026). *Morin: A Comprehensive Review of Its Sources, Nutraceutical Prospects, Chemistry, and Pharmacological Insights*. Phytotherapy Research.

Lee, H., Park, H. Y., & Jeong, T. S. (2021). Pheophorbide a derivatives exert antiwrinkle effects on UVB-induced skin aging in human fibroblasts. *Life, 11*(2), 147.

Liu, D., Mao, Y., Ding, L., & Zeng, X. A. (2019). Dihydromyricetin: A review on identification and quantification methods, biological activities, chemical stability, metabolism and approaches to enhance its bioavailability. *Trends in Food Science & Technology, 91*, 586–597.

Lopes, C., Obando, J. M. C., TCd, Santos, Cavalcanti, D. N., & Teixeira, V. L. (2024). Abiotic factors modulating metabolite composition in brown algae (phaeophyceae): ecological impacts and opportunities for bioprospecting of bioactive compounds. *Marine Drugs, 22*(12), 544.

Mahmoudi, M. R., Heydari, M. H., Qasem, S. N., Mosavi, A., & Band, S. S. (2021). Principal component analysis to study the relations between the spread rates of COVID-19 in high risks countries. *Alexandria Engineering Journal, 60*(1), 457–464.

Matos, ÂP (2017). The impact of microalgae in food science and technology. *Journal of the American Oil Chemists' Society, 94*(11), 1333–1350.

Matyash, V., Liebisch, G., Kurzchalia, T. V., Shevchenko, A., & Schwudke, D. (2008). Lipid extraction by methyl-tert-butyl ether for high-throughput lipidomics. *Journal of Lipid Research, 49*(5), 1137–1146.

Mhlongo, M. I., Piater, L. A., Steenkamp, P. A., Labuschagne, N., & Dubery, I. A. (2020). Metabolic profiling of PGPR-treated tomato plants reveal priming-related adaptations of secondary metabolites and aromatic amino acids. *Metabolites, 10*(5), 210.

Miller, G. L. (1959). Use of dinitrosalicylic acid reagent for determination of reducing sugar. *Analytical Chemistry, 31*(3), 426–428.

Munir, M., Khan, A. M., Qureshi, R., Murtaza, S., & Munazir, M. (2020). Preliminary phytochemical screening, proximate analysis, antioxidant and antibacterial activities of an algal species of Hydrodictyon reticulatum. *Journal of Bioresource Management, 7*(4), 1.

Nagappan, S., Devendran, S., Tsai, P-C, Jayaraman, H., Alagarsamy, V., Pugazhendhi, A., & Ponnusamy, V. K. (2020). Metabolomics integrated with transcriptomics and proteomics: Evaluation of systems reaction to nitrogen deficiency stress in microalgae. *Process Biochemistry, 91*, 1–14.

Nowicka, B. (2022). Heavy metal–induced stress in eukaryotic algae—mechanisms of heavy metal toxicity and tolerance with particular emphasis on oxidative stress in exposed cells and the role of antioxidant response. *Environmental Science and Pollution Research, 29*(12), 16860–16911.

Omololu, P. A., Rocha, J. B. T., & Kade, I. J. (2011). Attachment of rhamnosyl glucoside on quercetin confers potent iron-chelating ability on its antioxidant properties. *Experimental and Toxicologic Pathology, 63*(3), 249–255.

Othman, M. A., Yuyama, K., Murai, Y., Igarashi, Y., Mikami, D., Sivasothy, Y., … Monde, K. (2019). Malabaricone C as natural sphingomyelin synthase inhibitor against diet-induced obesity and its lipid metabolism in mice. *ACS Medicinal Chemistry Letters, 10*(8), 1154–1158.

Poovitha, S., & Parani, M. (2016). In vitro and in vivo α-amylase and α-glucosidase inhibiting activities of the protein extracts from two varieties of bitter gourd (Momordica charantia L.). *BMC Complementary and Alternative Medicine, 16*(Suppl 1), 185.

Qin, L., Wang, Z., Sun, Y., Shu, Q., Feng, P., Zhu, L., Xu, J., & Yuan, Z. (2016). Microalgae consortia cultivation in dairy wastewater to improve the potential of nutrient removal and biodiesel feedstock production. *Environmental Science and Pollution Research, 23*(9), 8379–8387.

Ramakrishnan, B., Megharaj, M., Venkateswarlu, K., Naidu, R., & Sethunathan, N. (2010). The impacts of environmental pollutants on microalgae and cyanobacteria. *Critical Reviews in Environmental Science and Technology, 40*(8), 699–821.

Re, R., Pellegrini, N., Proteggente, A., Pannala, A., Yang, M., & Rice-Evans, C. (1999). Antioxidant activity applying an improved ABTS radical cation decolorization assay. *Free Radical Biology and Medicine, 26*(9–10), 1231–1237.

Safafar, H., Van Wagenen, J., Møller, P., & Jacobsen, C. (2015). Carotenoids, phenolic compounds and tocopherols contribute to the antioxidative properties of some microalgae species grown on industrial wastewater. *Marine Drugs, 13*(12), 7339–7356.

Sharifi-Rad, M., Mohanta, Y. K., Pohl, P., Jaradat, N., Aboul-Soud, M. A., & Zengin, G. (2022). Variation of phytochemical constituents, antioxidant, antibacterial, antifungal, and anti-inflammatory properties of Grantia aucheri (Boiss.) at different growth stages. *Microbial Pathogenesis, 172*, Article 105805.

Sharifi Rad, J., Hoseini Alfatemi, S. M., Sharifi Rad, M., & Iriti, M. (2014). Free radical scavenging and antioxidant activities of different parts of Nitraria schoberi L. *Journal of Biologically Active Products from Nature, 4*(1), 44–51.

Sharma, J., Kumar, V., Kumar, S. S., Malyan, S. K., Mathimani, T., Bishnoi, N. R., & Pugazhendhi, A. (2020). Microalgal consortia for municipal wastewater treatment–Lipid augmentation and fatty acid profiling for biodiesel production. *Journal of Photochemistry and Photobiology B: Biology, 202*, Article 111638.

Silva, M., Geada, P., Pereira, R. N., & Teixeira, J. A. (2025). Microalgae biomass–A source of sustainable dietary bioactive compounds towards improved health and well-being. *Food Chemistry Advances*, Article 100926.

Stonik, V. A., & Stonik, I. V. (2018). Sterol and sphingoid glycoconjugates from microalgae. *Marine drugs, 16*(12), 514.

Symolon, H., Bushnev, A., Peng, Q., Ramaraju, H., Mays, S. G., Allegood, J. C., … Merrill, A. H., Jr. (2011). Enigmol: a novel sphingolipid analogue with anticancer activity against cancer cell lines and in vivo models for intestinal and prostate cancer. *Molecular Cancer Therapeutics, 10*(4), 648–657.

Tessaro, L., da, Silva, Mutz, Y., de Andrade, J. C., Aquino, A., Belem, N. K. R., Silva, F. G. S., & CA, Conte-Junior (2023). ATR-FTIR spectroscopy and chemometrics as a quick and simple alternative for discrimination of SARS-CoV-2 infected food of animal origin. *Spectrochimica Acta Part A: Molecular and Biomolecular Spectroscopy, 285*, Article 121883.

Uyaguari-Diaz, M. I., Chan, M., Chaban, B. L., Croxen, M. A., Finke, J. F., Hill, J. E., Peabody, M. A., Van Rossum, T., Suttle, C. A., & Brinkman, F. S. (2016). A comprehensive method for amplicon-based and metagenomic characterization of viruses, bacteria, and eukaryotes in freshwater samples. *Microbiome, 4*(1), 20.

Vanitha, P., Uma, C., Suganya, N., Bhakkiyalakshmi, E., Suriyanarayanan, S., Gunasekaran, P., … Ramkumar, K.Á. (2014). Modulatory effects of morin on hyperglycemia by attenuating the hepatic key enzymes of carbohydrate metabolism and β-cell function in streptozotocin-induced diabetic rats. *Environmental Toxicology and Pharmacology, 37*(1), 326–335.

White, R., Jones, I., & Gibbs, E. (1963). Determination of Chlorophylls, Chlorophyllides, Pheophytins, and Pheophorbides in Plant Material a. *Journal of Food Science, 28*(4), 431–436.

Zhang, J., & Luo, X. (2022). Bioaccumulation characteristics and acute toxicity of uranium in Hydrodictyon reticulatum: An algae with potential for wastewater remediation. *Chemosphere, 289*, Article 133189.